AN INVESTIGATION OF OPTIMAL DESIGN OF HYBRID ELECTRIC VEHICLE WITH A STARROTOR ENGINE

A Dissertation

by

YANG WANG

Submitted to the Office of Graduate and Professional Studies of
Texas A&M University
in partial fulfillment of the requirements for the degree of

DOCTOR OF PHILOSOPHY

Chair of Committee,	Mehrdad Ehsani
Committee Members,	Mark Holtzapple
	Shankar Bhattacharyya
	Le Xie
Head of Department,	Miroslav M. Begovic

December 2015

Major Subject: Electrical Engineering

ABSTRACT

Fuel economy of conventional hybrid electric vehicles (HEVs) gets limited improvements because of constraints from conventional internal combustion engines (ICEs). Electric vehicles (EVs) have the disadvantage of requiring large battery packs onboard. To overcome these problems, an HEV with a StarRotor Engine to replace the conventional ICE as the main power plant, which allows for a small battery pack, is proposed. The goal of this research is to develop an optimal design for the StarRotor Engine–based hybrid electric vehicle (SR–HEV) with minimal battery pack. The three most popular hybrid electric drivetrains are parallel, series and series–parallel, and each is studied in this research. All of them are fully analyzed for the purpose of maximally enhancing fuel economy.

A dynamic programming algorithm for optimal control of a dynamic model is implemented. The optimal control associated with the energy management is solved explicitly for each virtual hybrid electric drivetrain. The solution of the optimal control problem shows how optimal energy management strategies are derived. The same process is applied to conventional ICE HEVs to get the fuel economy to compare with SR–HEVs. The simulation indicates that the SR–HEVs can significantly increase vehicle fuel economy, and a series-parallel hybrid electric drivetrain with electric variable transmission (EVT) can provide better fuel economy among those drivetrains. An optimal design methodology is also presented for SR-HEVs in regards to fuel economy.

A parametric study shows that the appropriate gear ratios can further improve the fuel economy for the SR–HEV with EVT.

DEDICATION

To my parents, my wife and my daughter.

ACKNOWLEDGEMENTS

I would like to express my appreciation to many people who have contributed to my work. First of all, I would like to thank my advisor Dr. Mehrdad Ehsani for his patience, support and guidance during my PhD study as well as my PhD life. Beyond numerous specific technical problems, he also helped me to find the way to face the challenges and opportunities in my life and to achieve the final goals. His profound knowledge, gentle personality and rigorous attitude toward research will benefit my career as well as my whole personal life.

Further, I would like to show my gratitude to other committee members. Many thanks to Dr. Mark Holtzzaple for his help and guidance for my research, and I also want to thank Dr. Shankar Bhattacharyya and Dr. Le Xie for their valuable comments and interest in this research work.

I want to thank my friends and colleagues and the department faculty and staff for their help in my PhD life from 2010 to 2015. They made my time at Texas A&M University a great experience, especially the fellow students in power electronics & motor drives laboratory.

Last, but not the least, I would like to express my gratitude to my family, my parents, Jincai Wang and Qiuling Yang, my parents in law, Yijun Wang and Jingke Hu, my wife Xi Wang and my daughter Catherine Wang, for their continuous love and support for me. Their patience and abundant love are my endless source of motivation.

TABLE OF CONTENTS

Page

Page

LIST OF FIGURES

Page

Page

Page

LIST OF TABLES

Page

CHAPTER I

INTRODUCTION

This chapter introduces background and previous research on transportation electrification. The aim is to investigate fuel economy of the StarRotor Engine based Hybrid Electric Vehicles (SR–HEVs) with minimal size battery pack. The research objective is explained in this chapter to identify the originality of the work in the dissertation. The structure and organization of the dissertation are introduced at the last part of this chapter.

1.1 Background of the transportation electrification

Vehicles with Internal Combustion Engine (ICE) are facing more and more criticism for inefficient fuel consumption and air pollution with greenhouse gas emissions. The maximum efficiency of ICE is 30–35%. In other word, about 65–70% of thermal energy released by the fuel consumed is wasted as heat without being turned into any propulsion work or other useful work. The ICEs suffer from small maximum efficiency operation area, and the efficiency of the other operation area is much lower than the maximum one. The nitrogen oxides, carbon monoxide and carbon dioxide also come from ICE operation due to the combustion of hydrocarbon fuel [1].

In order to have vehicle with higher efficiency and cleaner emissions, vehicle development has not been stopped. Hybrid electric vehicles (HEV), which combines an ICE and electric motor, was invented in 90s last century. Compared with conventional

automobiles, the major benefit of HEVs is fuel economy because of the additional operating modes, which keep ICEs operating at higher efficiencies for most of the time [1]. The additional operation modes are 1) regenerative breaking, 2) engine operating points shifting, 3) engine driving operation, 4) pure electric driving.

There are three most popular ICE based hybrid electric drivetrain topologies, which are series, parallel and series–parallel. The series–parallel hybrid electric drivetrain is most promising because of its high fuel economy about 50 miles per gallon (MPG). However, the conventional ICE constrains still limits the further improvement of fuel economy for the conventional ICE based HEV.

In order to overcome the conventional ICE constrains, people are paying more and more attention to Electric vehicle (EV), which is mainly composed of electric traction motor and heavy pack of lithium batteries or fuel cells with ultracapacitors as energy sources. Without the ICE, EV can be propelled quietly and smoothly by using the electric motor whose efficiency is as high as 90%, which is much higher than ICE and fuel tank. The fuel economy can achieve around 100 miles per gallon gasoline equivalent (MPGe) [2]. Although fuel economy almost gets doubled compared to the conventional ICE based HEV, the huge battery packs of lithium battery, the most promising energy storage technology so far, bring many issues to EV. First of all, the EV price is still too expensive because of the high cost for lithium battery production and energy management. Secondly, the lithium battery pack is designed as the only onboard energy source in EVs, however, the power density and energy density of lithium battery are much less than ICE and fuel tank. Therefore these disadvantages of the lithium

battery cause the EV to have very limited travel range, long recharging time, and high cost. Taking Tesla for example, according to EPA report [2], the travel range of the Tesla with 85 kWh capacity lithium batteries is 265 miles. The normal charging regain is about 3 miles range per hour with standard household outlet [3], the dual DC charger offers 20 kW to fast charge the battery with the battery's lifetime damage. Therefore none of the travel range, recharging time and vehicle cost is satisfied compared to conventional vehicle with the refuel fuel tank.

The Plug–in HEV (PHEV) is just another version of HEV with a bigger size battery pack. For a short travel range the fuel economy can achieve as high as EV [4][5][6], because the design concept of PHEV is to use the battery energy as EV at beginning. The small size engine will take care of propulsion and charging after the battery depleted. The fuel economy is similar as Prius hybrid after the battery depleted [1][4]. Therefore the PHEV is a tradeoff product between HEV and EV.

1.2 Objectives of this dissertation

This dissertation aims at developing and designing a high fuel economy HEV with minimized battery pack. As discussed before, the existing solutions have their own limitations. We propose that StarRotor Engine [7], a novel rotary Brayton Cycle engine invented and patented by Dr. Mark Holtzapple from the Chemical Engineering Department of Texas A&M University, can be considered as an alternative to replace the conventional ICE as the main power source for automotive. A SR–HEV with the minimized the battery pack is proposed.

The StarRotor Engine's unique characteristics require hybrid electric drivetrain to further improve the fuel economy [7]. In order to fully investigate SR–HEV fuel economy, the three most popular HEV hybrid electric drivetrain topologies with optimal sizing design of the components will be explained in detail, and then these three hybrid electric drivetrains will be simulated with StarRotor Engine to fully investigate their fuel economy.

The implementation of the dynamic programming algorithm for optimal control of a dynamic model is explained. The optimal control associated with the energy management is applied to each virtual hybrid electric drivetrain on different driving cycles to fully investigate the fuel economy potential. The comparison between the fuel economies of each hybrid electric drivetrain with the StarRotor Engine will be performed and the result indicates the best fuel economy hybrid electric drivetrain for the SR–HEV among the hybrid electric drivetrains tested in this research. The same process applies to conventional ICE based HEVs to compare with the SR–HEVs for verifying the improvement.

A parametric study shows an appropriate transmission gear ratio can further improve the fuel economy for this StarRotor based series–parallel HEV with Electric Variable Transmission (EVT). An optimal design methodology is also developed to improve the fuel economy for SR–HEV.

1.3 Dissertation organization

This dissertation presents a systemic methodology for investigating fuel economy of the SR–HEVs with minimal size battery pack by using dynamic programming. The chapters are organized as follows:

The StarRotor Engine is introduced in Chapter II.

In Chapter III, the three most popular hybrid electric drivetrains are reviewed based on dynamic model.

Chapter IV explains the implementation of the dynamic programming algorithm for optimal control of a dynamic model developed for HEVs. This algorithm is used to calculate the maximum fuel economy with optimal control sequence for each hybrid electric drivetrain models on typical driving cycles.

Chapter V introduces the typical drive cycles and main components optimal design methodology for the three most popular HEV hybrid electric drivetrain topologies.

In Chapter VI, the SR–HEVs with different drivetrains are simulated by the dynamic programming for the fuel economy. Based on the same process, the conventional ICE based HEVs are also simulated. The comparison between the fuel economy results is made.

In Chapter VII, a parametric study shows the appropriate transmission gear ratios can further improve the fuel economy for series–parallel EVT drivetrain topology.

CHAPTER II

STARROTOR ENGINE

The StarRotor Engine was invented and patented by Dr. Mark Holtzapple from the Chemical Engineering Department of Texas A&M University, the proposed StarRotor Engine perfectly meets the most requirements for automobiles, and its properties are shown in following [8]:

- Efficient
- Power dense
- Low maintenance
- Long life
- Multi–fuel
- Quiet
- Small thermal signature
- Vibration free
- Low cost
- Low pollution

Compared with existing power source technologies for automobiles, the StarRotor Engine has potential to be considered as a main power source in HEV due to its unique features. Table 1 shows the existing power source technologies with serious limitations.

Table 1 Existing power source technologies for automobiles

Power Source	Disadvantages
Gasoline	Inefficient, vibrational, narrow range of fuel, and high pollution exhaust.
Diesel	Noisy, dirty, vibrational, narrow range of fuel and emit an unacceptable thermal signature.
Lithium battery	Low energy density, low power density, high pollution producing process and extra high cost.
Fuel cell	Hydrogen fuel required which is difficult to make and difficult to seal.
Gas turbines	Extremely high operation speed required, inefficient when operated off the design conditions, noisy, expensive and highly filtered air required.

2.1 StarRotor Engine construction and operation

Figure 1 shows a schematic of a StarRotor Engine [8]. Ambient air is compressed and directed to a heat exchanger that preheats the compressed air. The preheated air goes into a combustor where fuel is ignited to obtain the desired expansion temperature. The multi–fuel combustor can be used to release the thermal energy with little pollution. The hot compressed air flows to an expander where thermal energy is converted to shaft work. A portion of the shaft work is invested in the compressor, and the remaining

portion accomplishes useful work. The hot exhaust gases from the expander are sent to the heat exchanger where they are cooled and then discharged. Because the exhaust gas is cool, the thermal signature is small.

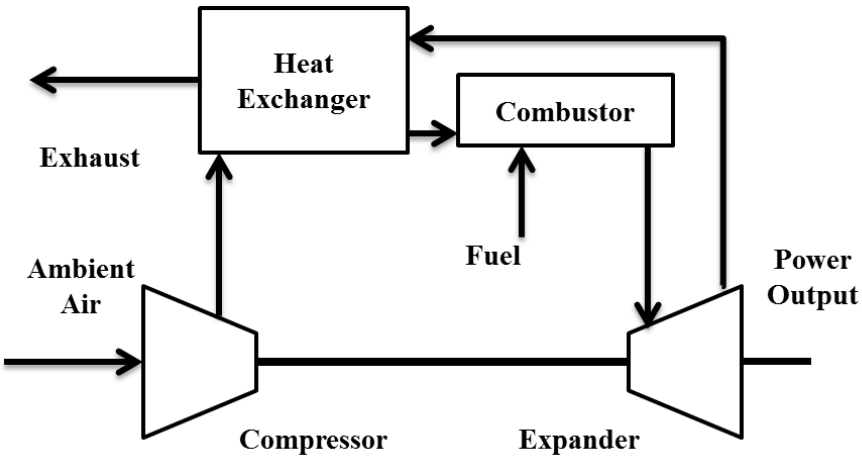

Figure 1 Schematic of StarRotor Engine.

Because of the high power density feature, Brayton Cycle Engines are famous for being applied to propel jet aircraft [8]. Compared with Otto and Diesel engines, which have a lower power density but also release high-pressure air to the environment with very loud noises from the throttling, the Brayton Cycle Engine can minimize the mechanical noises by releasing the exhaust gas at 1atm.

The dynamic compressor and expander are necessary for Brayton Cycle Engines because large volumes of air are required to achieve the desired power output. However, the traditional devices required extremely high rotational speed around 100,000 RPM to reach the pressure [8]. This extremely high rotational speed is the key for the operation efficiency. If the operation rotational speed is lower than this design speed, the

efficiency will drop dramatically. Further, the humidity and altitude will result in the changes in air density which also affects the operation efficiency.

In order to overcome the problems of common positive displacement compressors and expanders, the gerotors are designed to be applied to both the compressor and expander in the StarRotor Brayton Cycle engine [9][10].

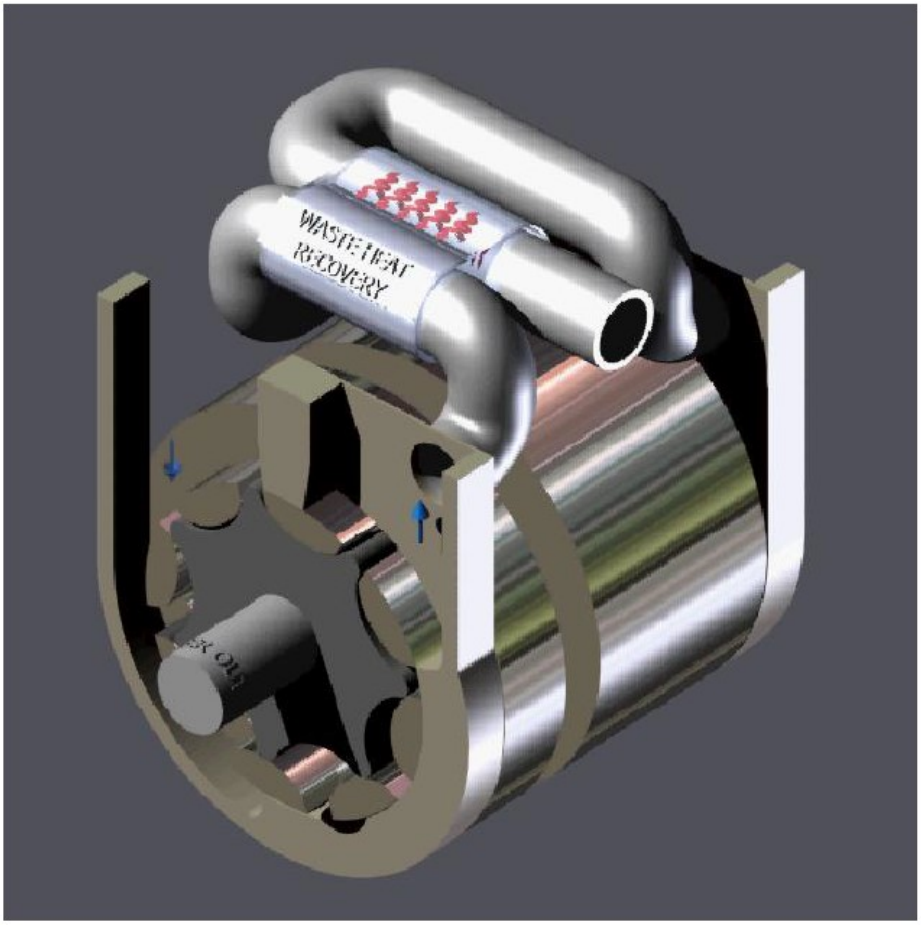

Figure 2 Reprinted figure from Ref. [10]. Three dimension schematic of the StarRotor Engine.

The three dimension schematic of the StarRotor Engine is shown in Figure 2. There is an inner gerotor with seven teeth and an outer gerotor with eight teeth in the StarRotor compressor [10]. As the gerotors rotate, the air is draw into the void when it opens through the inlet port, then the air is compressed when the void get closed.

The expander has the reverse operations to the compressor. As the gerotors rotates, the high pressure gas, which gets in through the inlet port, expands until the pressure reduces to 1 atm, and then the gas exhausts through the outlet port.

Because of the high temperatures in the operation of the Brayton Cycle Engine, the gerotors can't use the lubricants. Therefore no physical contact between the inner and outer gerotors is necessary in order to prevent friction [9]. The inexpensive surface treatment is required to reduce the gas leakage through the small gap. Because there is no physical contact, the maintenance is much easier and the longer life and higher reliability of the engine are expected.

2.2 Properties of a StarRotor Engine

According to [8], based on assumption material was silicon carbide embedded with randomly oriented carbon fibers and a few case studies with scaling laws used to extrapolate to the other engines the properties of StarRotor Engine are estimated and summarized in Table 2.

The StarRotor Engine can be designed within a wide range, for automobiles power rating application, the power rating is about 80 kW which could either belong to the low-power engine employs a single stage that compresses ratio from 1 to 6 or

medium power engine employ a two stage that compresses ratio from 6 to 36. The maximum rotational speed is limited by the stress from outer rotor in compressor or expander, therefore in this study the 80 kW StarRotor Engine is assumed to be a single stage one whose maximum speed is assumed to be 13,500 revolutions per minute (RPM).

Table 2 Reprinted table from Ref. [8]. Properties of the StarRotor Engines

Stage	Power [kW]	D [cm]	L [cm]	A	Speed [RPM]	m [kg]	P/m [kg/kg]
1	5	6.3	25.7	4	32,800	2.77	1.8
1	50	10.6	137	13	20,000	41.6	1.2
1	500	31.8	413	13	6,800	1,136	0.4
1	5,000	74	1,560	21	2,950	23,530	0.2
2	50	9.6	91	9	21,800	22	2.3
2	500	20	425	21	10,750	452	1.1
2	5,000	45	1,820	40	4,750	10,288	0.5
3	5,000	36	1210	33	6,000	4,267	1.2
3	50,000	80	4,409	46	2,300	110,491	0.46

Based on data from [7][9], the compressor torque is nearly constant, and the torque from the expander is also nearly constant. The engine torque will be nearly constant as well because both torque from compressor and expander are nearly constant

for a given compression ratio. For a preset pressure ratio design, if the pressure ratio varies away from the design pressure ratio, the trajectory of isentropic efficiency at the same operation speed will drop. The volumetric efficiency improves with increasing operation speed because leakage becomes a smaller portion of the total gas flow. The efficiency of the StarRotor Engine depends on the combustor temperature and compressor/expander operation efficiency. Compressor and expander efficiency are very important factors for operation efficiency of StarRotor Engine. However, there is not enough data to indicate the relation between operation torque and pressure ratio. Therefore, a StarRotor Engine with a given pressure ratio is assumed in this research. Thus operation torque is hypothesized to keep nearly constant during all operation speed range, and its efficiency is from 60–65% as a linear function of operation speed [9][10]. The high operation temperature is another key factor for StarRotor Engine's high efficiency performance. However, in order to reach the required temperature from ignition the StarRotor Engine needs 120 second to startup. These are main reasons why the hybrid electric drivetrain is necessary for StarRotor Engine vehicle. The torque and power of StarRotor Engine are represented in Figure 3.

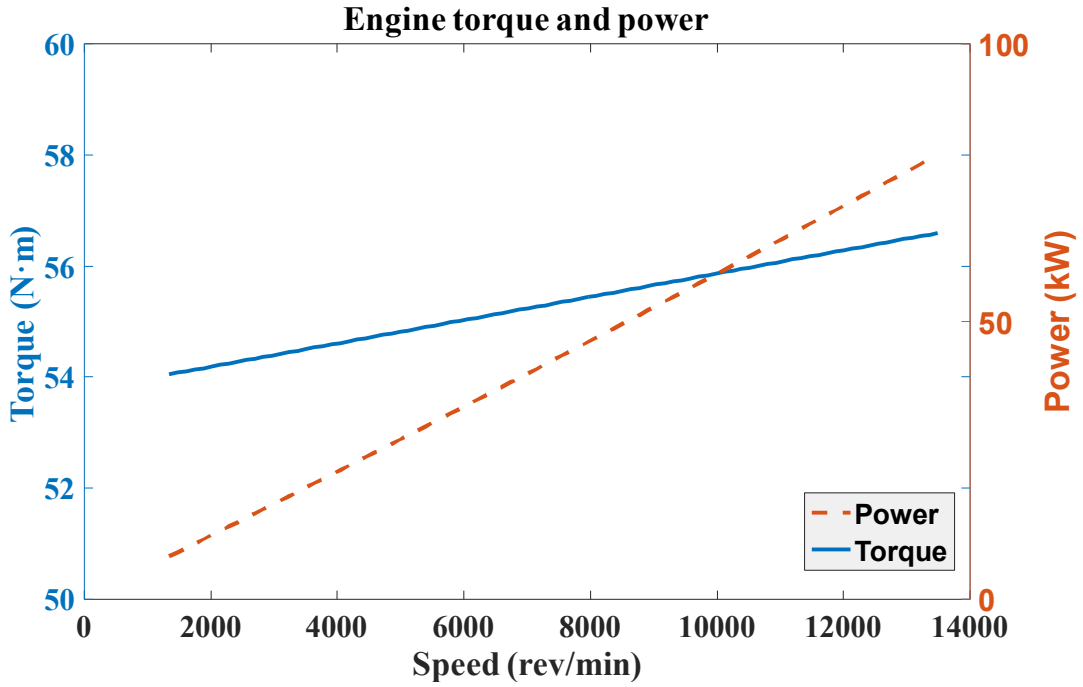

Figure 3 Engine torque and power for the 80 kW StarRotor Engine.

2.3 Summary

In this chapter, the StarRotor Engine is briefly introduced, this novel StarRotor Engine not only provides higher maximum operation efficiency but also offers much wider high operation efficiency range. However, this engine has to wait about 120 seconds in order to reach designed operating temperature and only operate at nearly constant torque.

Since the assumed StaroRotor engine is a high rotational speed and low mechanical torque output Brayton Cycle engine, this research in following chapters will use dynamic programming to analyses SR–HEVs with different hybrid electric

drivetrain to compare fuel economy in order to find out the best fuel economy hybrid electric drivetrain topology.

CHAPTER III

VEHICLE DYNAMIC AND HYBRID ELECTRIC DRIVETRAIN COMPARISON

A vehicle is a complex system that includes thousands of components. Vehicle behavior can be described mathematically by the vehicle operation based on the general physical principles. In this chapter, the vehicle dynamic fundamentals will be reviewed, and the conventional drivetrain and the three most popular hybrid electric drivetrains will be explained.

3.1 Vehicle dynamics

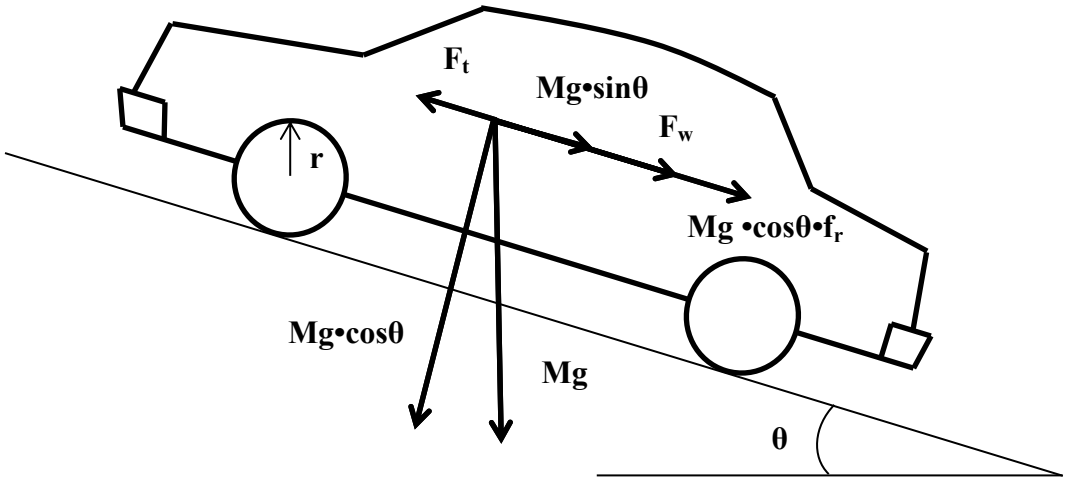

Figure 4 Forces acting on a vehicle.

All forces acting on the vehicle in the driving direction will determine the vehicle's movement behavior. As shown in Figure 4, the tractive effort F_t, which is

produced by the onboard power plant torque output transmitted to driven wheels, propels the vehicle forward.

The vehicle resistances, which are trying to stop the vehicle movement, includes rolling resistance of the tires, appearing in Figure 4 as rolling resistance force $Mg{\cdot}f_r{\cdot}Cos\theta$, aerodynamic drag, F_w, and hill climbing resistance, which is the term $Mg{\cdot}Sin\theta$ [1].

And the dynamic model of the vehicle based on the driving load power is expressed as

$$P_{load} = V \cdot (Mg \cdot f_r + \frac{1}{2}\rho_a \cdot C_D \cdot V^2 + Mg \cdot \sin i) + M\delta \frac{dV}{dt} \qquad (3.1)$$

where M is the vehicle mass, f_r is the rolling resistance coefficient, ρ_a is the air density, C_D is the aerodynamic drag coefficient, A_f is the front area, V is the vehicle speed, θ is the grade of the road, and δ is rotational inertia factor, which converts the inertia of the rotating components to the mass. The first term of equation 3.1 is for the resistance, and the last term is for the vehicle acceleration [1]. The parameters used in this research are listed in Table 3, the M_{pp} is the total weight of the onboard power plant components which will be discussed in later chapter.

Table 3 The vehicle parameters

M (kg)	1300+M_{pp}
f_r	0.01
ρ_a(kg/m^3)	1.205
A_f(m^2)	2.0
C_D	0.3
δ	1.07

3.2 Drivetrain comparison

There are many drivetrains invented and used worldwide. The conventional drivetrain and the three most popular hybrid electric drivetrains, series, parallel and series-parallel, are presented in this chapter.

3.2.1 Conventional drivetrain

In conventional drivetrain, the engine is connected to the wheels via the multi–gear box and final gear in order to follow the propulsion demand. The configuration of the conventional drivetrain is shown in Figure 5. It is necessary to have multi–gear which is able to change the ratio between engine speed and wheel speed to make sure the engine could follow the wheel demand for both the torque and speed. The equations for this hybrid electric drivetrain are shown as followed [1][11].

$$T_{eng} = \frac{T_{wheel}}{R_{final} \times R_{gear}} \tag{3.2}$$

$$\omega_{eng} = \omega_{wheel} \times (R_{final} \times R_{gear}) \tag{3.3}$$

$$P_{eng} = \omega_{eng} \times T_{eng} \tag{3.4}$$

where R_{gear} is the gear ratio for multi-gear box, R_{final} is the final gear ratio, T_{eng} is the engine torque, T_{wheel} is the torque from the wheel, ω_{eng} is the engine operating radians speed and ω_{wheel} is the wheel radians speed.

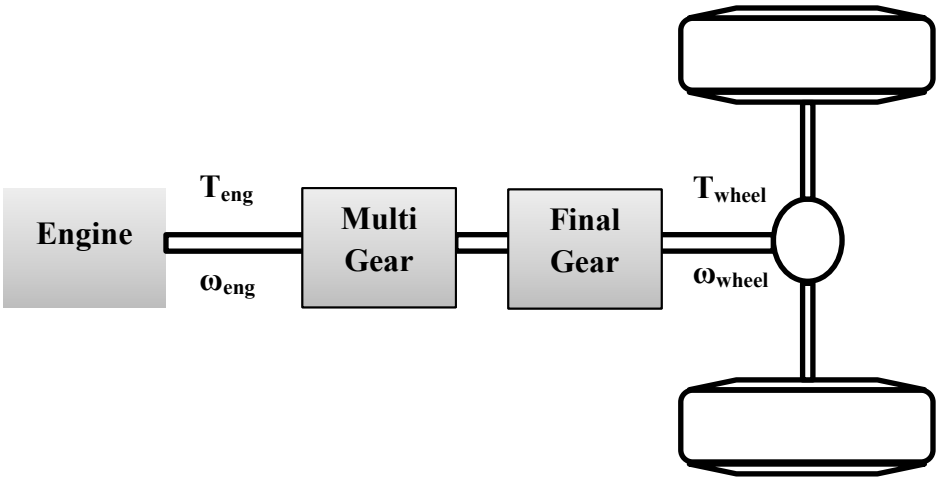

Figure 5 Schematic of a conventional drivetrain.

The engine is the only power source for propulsion. Pure mechanical braking will be used for properly and quickly reducing vehicle speed. Because of low fuel efficiency characteristics of operation points of conventional ICE during driving cycles and dissipation of vehicle kinetic energy during braking in conventional drivetrain, the main disadvantages of the conventional ICE vehicle are poor fuel economy and environmental pollution.

In order to improve the conventional drivetrain fuel economy, the hybrid vehicle, which equips two or more power trains, was invented. A hybrid vehicle with an electric power train is called hybrid electric vehicle (HEV). There are three most popular hybrid electric drivetrain topologies getting more and more attention.

3.2.2 Series hybrid electric drivetrain

The series hybrid electric drivetrain consists of an engine, a generator, energy storage (normally a battery pack) and a traction motor [1][12][13], as shown in Figure 6. In the series hybrid electric drivetrain, unlike the other hybrid electric drivetrain, there is no mechanical connection from engine to the wheels. Therefore, this is possible to operate engine decoupled from driven wheels torque and speed demand, which means engine operation efficiency is independent of the road torque and speed demand. The size of the battery is important because it is related to the control flexibility of the engine. A small battery requires an engine control that follows the demand power of the vehicle closely. If a large battery is used the engine can operate more independently of the road power demand, because the battery can be used for transient power demands. This hybrid electric drivetrain originally come from an EV whose travel range could be extended by adding the engine-generator as a power source to the EV drivetrain.

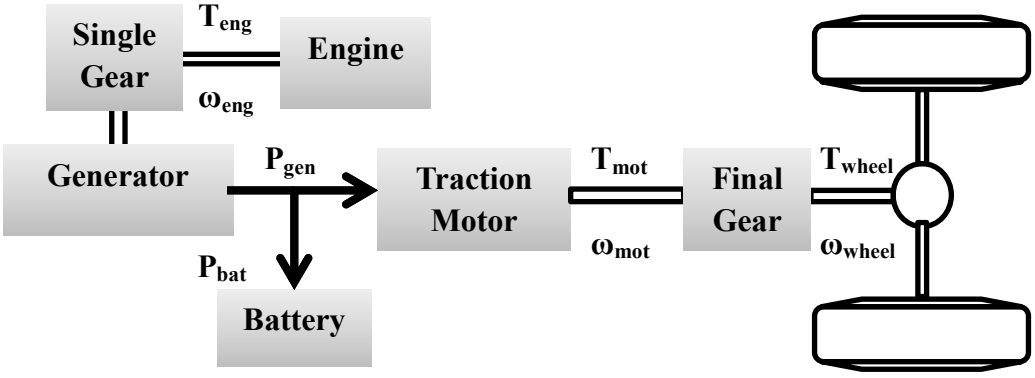

Figure 6 Schematic of a series hybrid electric drivetrain.

$$T_{mot} = T_{wheel} / R_{final} \tag{3.5}$$

$$\omega_{mot} = \omega_{wheel} \times R_{final} \tag{3.6}$$

$$T_{gen} = T_{eng} / R_{\sin} \tag{3.7}$$

$$\omega_{gen} = \omega_{eng} \times R_{\sin} \tag{3.8}$$

$$P_{bat} + P_{gen} = P_{mot} / \eta_{mot}^{sign(P_{mot})} \tag{3.9}$$

where R_{sin} is the gear ratio of single gear, R_{final} is the gear ratio of final gearbox, T_{eng} is the engine torque, T_{mot} is the traction motor torque, T_{gen} is the generator torque, T_{wheel} is the torque from the wheel, ω_{eng} is the engine operating radians speed, ω_{mot} is the traction motor radians speed, ω_{gen} is the generator operating radians speed and ω_{wheel} is the wheel radians speed.

The series hybrid electric drivetrain has five operation modes as follows [1],

- Pure electric traction mode:

  During this mode, the electric motor operates alone to propel the vehicle. Meanwhile the engine is shut down.

- Engine–generator alone traction mode:

  In this operating mode, only the engine–generator operates to supplies its required power from the traction motor.

- Hybrid propelling mode:

  Both of engine–generator and battery supply their powers to the electric motor drive.

- Battery charging from the engine–generator:

  In this case, the engine–generator has to supply the enough power to traction motor in order to follow the driven wheels demand but also provide power to charge the battery.

- Regenerative braking mode:

  The traction motor can be used as a generator in order to minimize the fuel economy by converting the kinetic energy of the vehicle mass to electric energy to charge the battery during the braking.

3.2.3 Parallel hybrid electric drivetrain

In the parallel hybrid electric drivetrain, the engine is mechanically connected to the wheels. A traction motor, as the second torque source, provides additional torque to help the engine follow the wheels demand. This traction motor can also work as a generator to collect the braking energy. A torque coupler, required in this specific hybrid electric drivetrain, is able to allow the engine and traction motor to constitute their mechanical torque in parallel directly to the driven wheels. As shown in Figure 7, this is a two-shaft configuration, in which two transmissions are used [1][13]. One is between the engine and the torque coupler as engine transmission, and the other is between the traction motor and the torque coupler as motor gear which is a fixed gear ratio. Both of the transmissions could be single or multi-gear. According to [1][14], the multi–gear engine transmission and single ratio motor gear could not only overcome the disadvantage of engine flat torque output in entire speed range and limited high efficient

operation area but also take advantage of the high torque output of traction motor at low speed.

Unlike series hybrid electric drivetrain, the parallel hybrid electric drivetrain not only has fewer energy conversions but also gets a significant fuel economy and performance improvement by using a small size traction motor and battery pack [15][16]. The major disadvantage is that the operation speed of engine and traction motor are out of control.

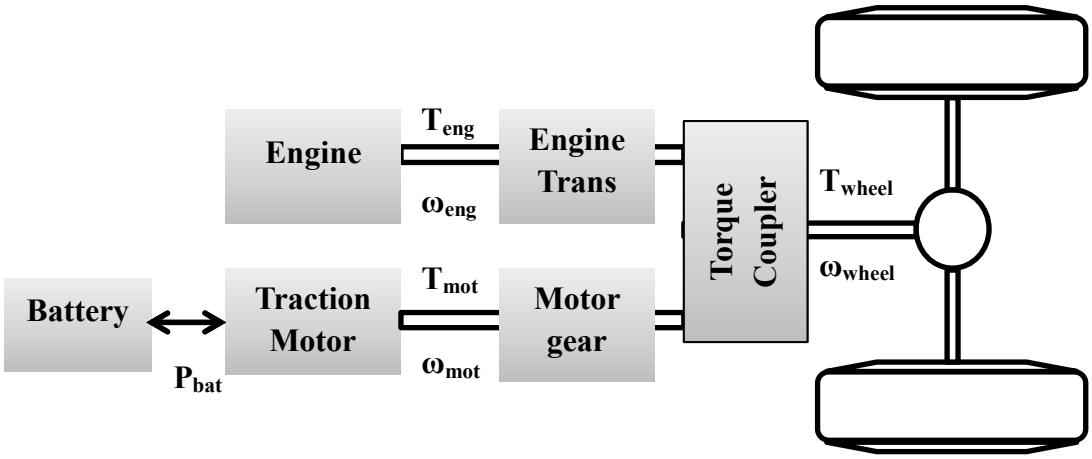

Figure 7 Schematic of a parallel hybrid electric drivetrain.

$$T_{eng} \times R_{eng} + T_{mot} \times R_{mot} = T_{wheel} \tag{3.10}$$

$$\omega_{eng} = \omega_{wheel} \times R_{eng} \tag{3.11}$$

$$\omega_{mot} = \omega_{wheel} \times R_{mot} \tag{3.12}$$

$$P_{eng} = \omega_{eng} \times T_{eng} \tag{3.13}$$

$$P_{mot} = \omega_{mot} \times T_{mot} \tag{3.14}$$

$$P_{bat} = P_{mot} / \eta_{mot}^{sign(P_{mot})} \quad (3.15)$$

where R_{eng} is the gear ratio of engine transmission, R_{mot} is the gear ratio of motor gear, T_{eng} is the engine torque, T_{mot} is the traction motor torque, T_{wheel} is the torque from the wheel, ω_{eng} is the engine operating radians speed, ω_{mot} is the traction motor radians speed, and ω_{wheel} is the wheel radians speed.

The parallel hybrid electric drivetrain has five operation modes as followes [1],

- Pure electric traction mode:

  During this mode, the electric motor alone propels the vehicle. Meanwhile the engine is shut down.

- Engine alone traction mode:

  In this operating mode, only the engine operates to supplies required power from the driven wheels.

- Hybrid propelling mode:

  Both engine and traction motor supply their torque to the driven wheels.

- Battery charging from the engine:

  In this case, the engine has to supply enough power to follow the driven wheels torque and speed demand but also provide power to charge the battery through the traction motor which operates as generator.

- Regenerative braking mode:

  The traction motor can be used as a generator in order to minimize the fuel economy by converting the kinetic energy of the vehicle mass to electric energy to charge the battery during the braking.

3.2.4 Series-parallel hybrid electric drivetrain

The series and the parallel hybrid electric drivetrains have their own advantages and disadvantages. In order to get the further improvement, a hybrid electric drivetrain, which combines the series and the parallel hybrid electric drivetrain advantages and eliminate their disadvantages, gets more and more attention [17]18].

The Figure 8 shows the most famous example of series–parallel hybrid electric drivetrain, Toyota Hybrid System (THS), which uses a planetary gearbox to couple the torque and speed with two electric machines by using generator to control the engine operation speed and traction motor to assistant the engine output torque through an axle gear as a torque coupler [19][20]. As shown in Figure 9, the engine connects to the carrier gear, the generator links to the sun gear and the output torque from the engine and the generator is acting on the ring gear. The pinion gears, which are between sun and the ring, rotate with the speed difference of those two gears. The ring gear and traction motor are connected to final gear via the torque coupler. In this hybrid electric drivetrain, the generator can be used to charge the battery when the planetary carrier is operated at higher rotational speed than the ring gear. The generator also can be locked, there is no electric power transmit to battery under this situation, the engine torque will directly propel the driven wheels via the ring gear like parallel hybrid electric drivetrain [21]. In electric mode only the traction motor is operating while the generator rotor is rotating at no-load, and the engine is at standstill. In hybrid propulsion mode, both of the generator and the traction motor are working at the same time, thus the battery will be charged or discharged depending on the difference between the traction motor power

demand and generator output power. The generator breaks the ICE's power, one part, as mechanical power, directly delivers to driven wheels, and the other part, through generator, is transmitted to the battery as electric power[22][23]. The generator can adjust the speed of the sun gear in order to keep ICE running at a rotational speed with higher efficiency while the traction motor contributes to the torque management as the similar way.

The engine torque must be balanced in planetary gear in order to transmit torque from the engine (planetary carrier) to the output as shown.

$$T_{\text{gen}} = -T_{eng} \times \frac{R_{\text{planeray}}}{1 + R_{\text{planeray}}} \tag{3.16}$$

where $R_{planetary}$ is the ratio of between the sun gear teeth number and the ring gear teeth number.

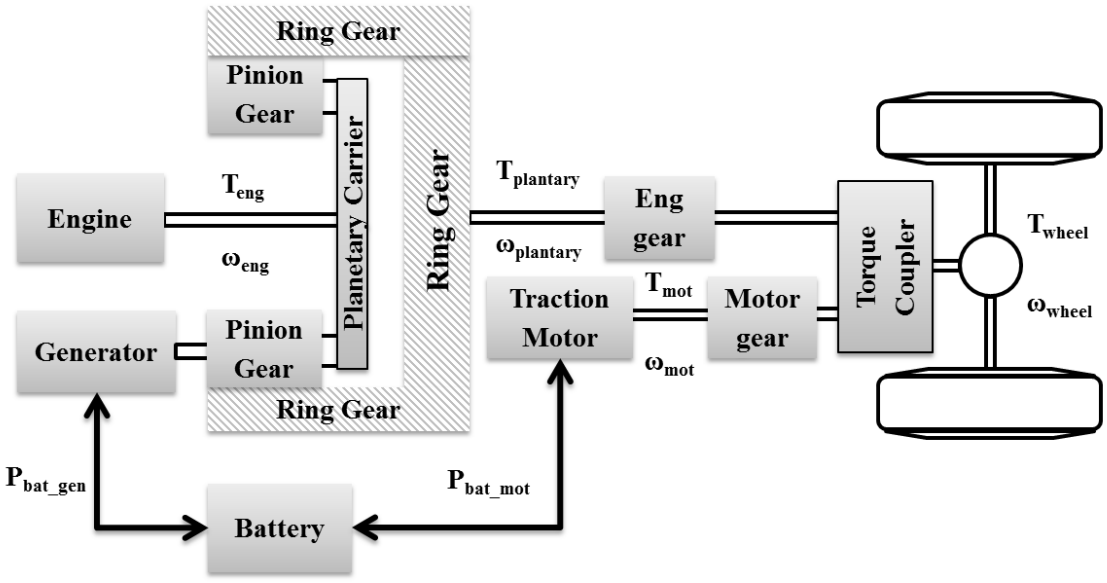

Figure 8 Schematic of a series–parallel planetary gear hybrid electric drivetrain.

.

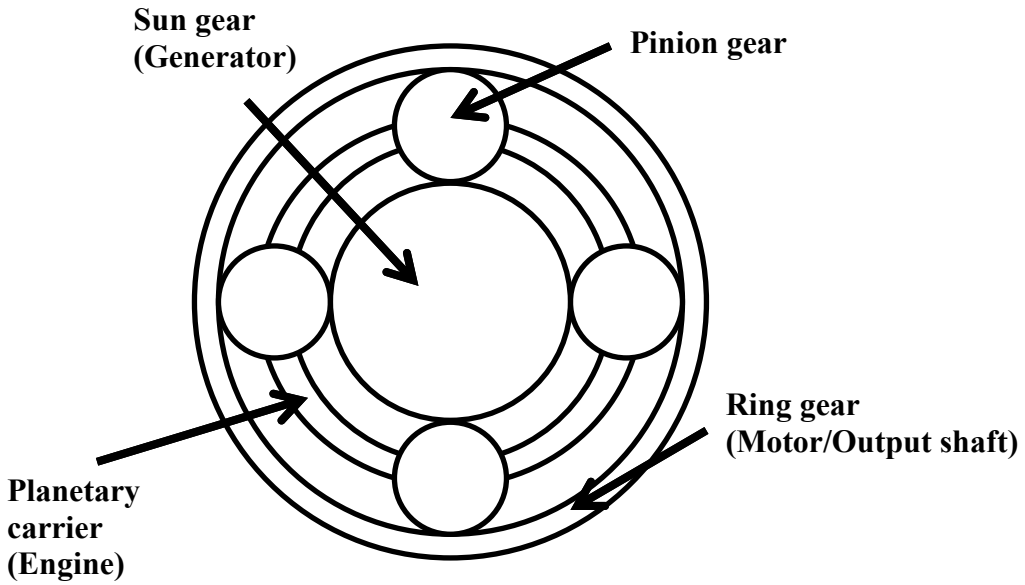

Figure 9 Schematic of a planetary gear.

Besides the THS, there is another type of series–parallel hybrid electric drivetrain called Electric Variable Transmission (EVT) which constitutes one double rotor machine (DRM) and one conventional machine as shown in Fig.10. The DRM consists of the outer rotor with windings fed through the slip rings and the inner rotor with permanent magnets [24][25]. This DRM with extra traction motor, which has the very similar functionality as THS without the clutch or complicated planetary gearbox, allows the engine to operate at the efficient operating points in order to maximize the system efficiency or minimize the whole driving cycle fuel consumption [26][27][28]. The DRM can either increases or decreases the engine operation speed to meet the rotating speed demand at the driven wheels. The traction motor is able to increase or decrease the torque of the engine to the track the required torque demand from driven wheels. This

hybrid electric drivetrain also has the capability to operating in a pure electric mode as EV [29].

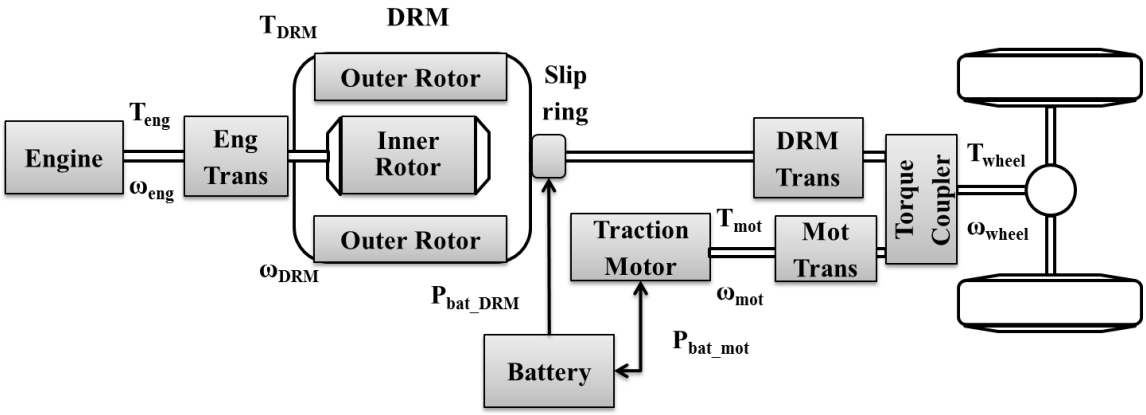

Figure 10 Schematic of a series-parallel EVT hybrid electric drivetrain.

As shown in Figure 10, the engine connects to the shaft of the inner rotor via a single–gear box named engine gear and driven wheel shaft connects to the outer rotor via another single–gear box named DRM gear. The relative rotational speed difference between the inner and outer rotor is controlled by the applied voltage and frequency in winding of the outer rotor. In steady–state, the torque on the outer rotor is as same as the inner rotor torque. Therefore, if the inner rotor can rotate faster than outer rotor, the DRM generates positive power to DC bus when, if inner rotor rotates slower than outer rotor, the electric power is delivered to DRM from DC bus [30].

Because the inner and the outer rotor of DRM should be in agreement with torque balance, the engine output torque transmitted to the inner rotor of DRM should be

balanced with DRM outer rotor torque which is as same as DRM mechanical output torque.

Therefore the power produced by the engine P_{eng} is divided into two parts at the DRM, the electric power P_{bat_DRM} either generated from DRM which delivers to DC bus or extracted from DC bus to DRM, in either way, the rest power is the mechanical power transmitted from DRM to the driven wheels through the DRM gear [31].

$$\omega_{\text{mot}} = \omega_{\text{wheel}} \times R_{\text{mot}} \tag{3.17}$$

$$\omega_{\text{outer}} = \omega_{\text{wheel}} \times R_{\text{DRM}} \tag{3.18}$$

$$\omega_{\text{inner}} = \omega_{\text{eng}} / R_{\text{eng}} \tag{3.19}$$

$$T_{mot} \times R_{mot} + T_{DRM} \times R_{DRM} = T_{wheel} \tag{3.20}$$

$$\omega_{\text{DRM}} = \omega_{inner} - \omega_{\text{outter}} \tag{3.21}$$

$$T_{eng} = T_{DRM} / R_{eng} \tag{3.22}$$

$$R_{eng} \in [\frac{\max(T_{eng})}{\max(T_{DRM})}, \frac{\max(\omega_{eng})}{\max(\omega_{DRM})}] \tag{3.23}$$

$$R_{DRM} \in [\frac{\omega_{DRM\_base}}{\max(\omega_{wheel})}, \frac{\max(\omega_{DRM})}{\max(\omega_{wheel})}] \tag{3.24}$$

where the ω_{DRM_base} is the base speed of the DRM, ω_{DRM} and T_{DRM} are the DRM operation speed and torque, ω_{inner} and ω_{outer} are the inner and outer rotor rotational speed, R_{mot}, R_{DRM} and R_{eng} are the motor, DRM and engine gear ratios respectively.

The operation modes of this series-parallel hybrid electric drivetrain are [32]:

- Pure electric traction mode:

  In the pure electric propulsion mode, the engine is turned off and the outlet shaft is the locked, thus there is no rotational speed on the inner rotor. The outer rotor rotates with the synchronous speed determined by the driven wheels rotational speed and motor gear ratio. The traction motor provides required torque to follow the driven wheels torque demand.

- Engine alone mode:

  In engine only traction mode, the engine would follows the torque and rotational speed demand from the driven wheels through the DRM gear.

- Engine operation with assistance from machines mode:

  During this mode, the engine is delivering power to the driven wheels, and both of the traction motor and DRM operates to assistant the engine to follow the driven wheels demands. The battery output power is used to balance the power of two electric machines depended on the control strategy. This mode could be used most of time because of the capability to handle most road condition with optimal fuel consumption.

- Regenerative braking:

  In regenerative braking mode, the traction motor is performed as a generator. The brake torque, applied on the traction motor, would provide negative torque on traction motor to generate the negative power, which is delivered to the battery and charge it.

There are four possible operation modes when both electric machines working at same time which is different from other hybrid electric drivetrains described as [33]:

- Increased speed and torque: the battery provides power to both machines to increase the torque and speed to meet demands from driven wheels.
- Decreased speed and increased torque: the DRM operates as generator to decrease the engine speed and traction motor helps engine to increases the torque for meeting demand.
- Decreased speed and torque: Both machines are operating as generator to charging the battery pack.
- Increased speed and decreased torque: the DRM operates to increase the engine rotational speed and the traction motor operates as generator.

3.3 Summary

Four different drivetrains are introduced and analyzed based on the vehicle dynamic knowledge reviewed in this chapter. Except conventional drivetrain, the three hybrid electric drivetrains, which are parallel, series and series-parallel, have electric path to assistant the engine to follow the driven wheels demand in order to make engine operate in efficient operating area. After understanding these three hybrid electric drivetrains' characteristics, the following chapters will make fuel economy comparison between them in order to find the highest fuel economy hybrid electric drivetrain for SR–HEV among them.

CHAPTER IV

DYNAMIC PROGRAMMING ON HEV

The dynamic programming is famous for calculating the optimal control sequences for any hybrid electric drivetrain in order to get the optimal overall fuel consumption. In this Chapter, the application of dynamic programming on any hybrid electric drivetrains is introduced.

4.1 Background

In order to lead to a minimal cost for the whole process, dynamic programming can be used to effectively solve the problems with input and state constrains and to fix the time window for optimal control sequences for systems [34][35]. Since the dynamic programming is a numerical algorithm, the discretization is necessary with the discrete-time model,

$$x_{k+1} = F_k(x_k, u_k) \qquad k = 0,1,\ldots,N-1 \tag{4.1}$$

where x is the state variable and u is the control signal, the disturbance is also required to be known perfectly in advance at every time instance.

The problem can be expressed as following

$$\min J_\pi(x_0) = C_N(x_N) + \sum_{k=0}^{N-1} h_k(x_k, u_k(x_k)) + \phi_k(x_k) \tag{4.2}$$

$$x_{k+1} = x_k + f_k(x_k, u_k) \tag{4.3}$$

$$x(0) = x_0 \tag{4.4}$$

$$x_N \in [x_{N,\min}, x_{N,\max}] \tag{4.5}$$

$$x_k \in X_k \tag{4.6}$$

$$u_k \in U_k \tag{4.7}$$

where the J is the cost function with the control sequences π, $C_N(x_N)$ is the final cost with the additional penalty forcing a partially constrained final state, $h_x(x_k,u_k(x_k))$ is the cost of applying the control u_k with the variable x_k at time instance k.

By proceeding backward in time, the dynamic programming is able to evaluate the cost function J which is minimized for each x^i at every time instance k,

$$J_k(x^i) = \min\{J_{k+1}(x^i, u_{k+1}) + h_k(x_k, u_k(x_k)) + \phi_k(x_k)\} \tag{4.8}$$

where $\phi_k(x_k)$ is the penalty function, and the line interpolation of the cost function $J_{k+1}(x^i,u_{k+1})$ is used. The controls of the equation 4.8 create an optimal control signal map which can be used in forward simulation of the same model with the same final state x_N to generate the optimal state trajectory.

Because the infeasible states and inputs are infinitely expensive and should have infinite cost, there are always some numerical errors that happen by using those infinite cost to calculate in the state space. In order to avoid these errors mentioned above with high accuracy, the paper [36] presents a method which can solve this problem at the boundary line between the feasible and infeasible regions. In one dimensional dynamic system problems, there exist two infeasible regions, upper and lower region respectively.

The lower boundary line is defined as the lowest state $x_{k,low}$ at each time instance k that allows achieving the minimal final state. The problem is initialized with minimal

final state. The lower boundary line can be evaluated by sequentially going backwards in time from $k = N$-1 to $k = 0$ and solving the following optimization process. At each time step, the $x_{k+1,low}$ is known, in order to get the $x_{k,low}$, the u_k is required to maximize the $f_k(x_{k,low},u_k)$ as shown in following equations. The upper boundary line is found analogously like lower boundary. After the boundary lines are evaluated, the feasible region only simulation can provide higher accuracy on control signal interpolation.

$$x_{k+1,low} = x_{k,low} + \max f_k(x_{k,low},u_k) \tag{4.9}$$

$$x_{k+1,up} = x_{k,up} + \max f_k(x_{k,up},u_k) \tag{4.10}$$

4.2 Dynamic programming on HEV

In order to calculate the minimal offline fuel consumption, dynamic programming is frequently applied to hybrid electric drivetrain on a pre-known driving cycle. Based on the models of onboard power plant components, the optimization goes upstream from the driven wheels to the battery pack and the StarRotor Engine with backward approach.

Instead of considering engine power or motor torque as the control variables in[14][20], in this research, the battery State-Of-Charge (SOC) is the only state variable, the battery output power can be considered as a control variable on any type of hybrid electric drivetrain. The maximum SOC values at each time instance is calculated by the up boundary line. In a HEV simulation, the final SOC always is as same as the initial value, the second up boundary line can be evaluated by sequentially going forward in time from $k = 1$ to $k = N$, the maximum SOC values at each time instance are the smaller

ones between the maximum SOC values of two boundary lines. The same idea takes place for the minimal SOC of low boundary. The state-time grid is meshed in time and SOC which is sampled between the minimum and maximum SOC values $x_{k,min}$ and $x_{k,max}$ at each time instance as shown in Figure 11.

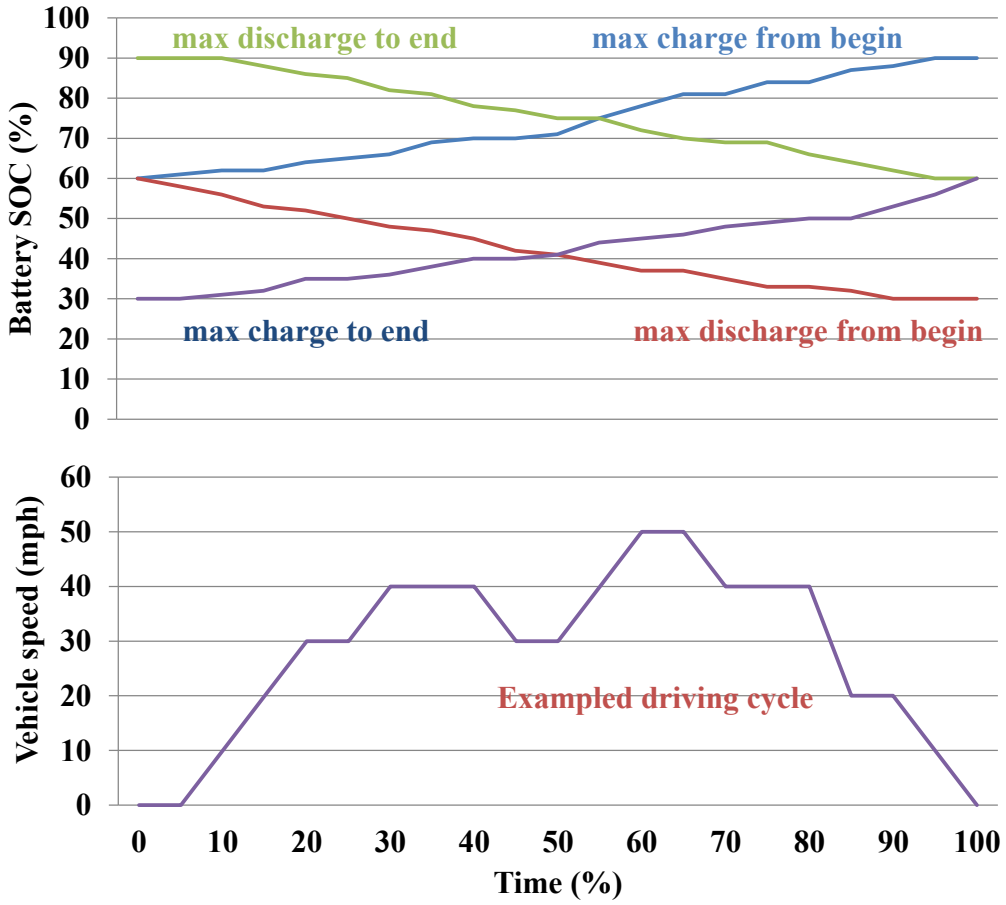

Figure 11 SOC variation based dynamic programming applied to HEVs.

The SOC constraints are not only limited by maximum battery charge or discharge current but also depend on the other electrical component model [37]. For example, in pure electric mode, the maximum battery discharge power maybe high

enough, however, it is possible that the traction motor is not powerful to convert all regenerative braking power. The maximum regenerative braking power limits the maximum battery charging power.

The principle is to find the control sequences to follow the optimal battery SOC trajectory which minimizes the total fuel consumption along a whole driving cycle known in advance [38]. The fuel consumption objective J can be stated as following

$$J = \sum_{k=0}^{N-1} h_k(x_k, u_k(x_k)) \cdot 1s \tag{4.11}$$

where J is the instantaneous fuel consumption between two consecutive time instances, the k is the fuel consumption.

The dynamic programming mentioned above can be applied to any HEV topology. For a different hybrid electric drivetrain, the control variable could be different. For example, the traction motor output torque can be also chosen as a control variable in parallel drivetrain; however, it is not compatible with a series hybrid electric drivetrain because the traction motor is the only propulsion components in this drivetrain. Therefore, in this study, the battery output power is chosen to be the control variable because the battery output power is easier to apply to all these three hybrid electric drivetrains without massive modification.

The operation modes category based on the state variable is shown in Table 4 for different drivetrains. If the driven wheels power demand is positive, the HEV operation modes can be determined by the SOC difference between the time instance k and k+1, which are $x(k)$ and $x(k+1)$ namely. When the demand power is negative, the regenerative braking is used to recover the braking energy and charge it into the battery.

Table 4 Operation modes category based on the state variable changes

	$P_{wh,load} \geq 0$			$P_{wh,load} \leq 0$
	$x(k) > x(k+1)$	$x(k) = x(k+1)$	$x(k) < x(k+1)$	$x(k) < x(k+1)$
Parallel	Pure electric / Hybrid	Engine only	Charging with engine on	Regenerative braking
Series	Pure electric / Hybrid	Engine only	Charging with engine on	Regenerative braking
Series-Parallel	All modes but regenerative braking	Engine only/ Hybrid	All modes but regenerative braking	Regenerative braking

4.2.1 Parallel hybrid electric drivetrain

For a parallel hybrid electric drivetrain, the battery output power is determined by the traction motor operation whose operation modes include motor traction alone and hybrid [39]. When the energy flows from the battery to the driven wheels, the motor output power P_{mot} is positive, and can be expressed as:

$$P_{mot} = (x(k) - x(k-1)) \cdot Q_n \cdot \eta_{mot} \tag{4.13}$$

where Q_n is the energy capacity of the battery, η_{mot} is the efficiency of the traction motor.

The charging battery operation modes include regenerative braking and battery charging from the engine [40]. When the energy flows from the driven wheels to the battery, the motor power P_{mot} is negative,

$$P_{mot} = \frac{(x(k) - x(k-1)) \cdot Q_n}{\eta_{mot\_g}} \tag{4.14}$$

where η_{mot_g} is the efficiency of the traction motor operated as generator. The power consumed by engine is

$$P_{eng} = P_{load} - P_{mot} \tag{4.15}$$

where P_{load} is obtained from the driving cycle and onboard power plant component model. With battery energy capacity Q_n and the efficiency parameters, the engine power and motor power are determined fully by the SOC variation at each time interval k to k+1.

4.2.2 Series hybrid electric drivetrain

For series hybrid electric drivetrain, the battery pack output power is determined by the difference between the required power from traction motor and generator output power [41][42]. When the energy flows from the battery to the driven wheels, the traction motor output power P_{mot} is positive, and can be expressed as:

$$P_{mot} = (x(k) - x(k+1)) \cdot Q_n + P_{e\_g}) \cdot \eta_{mot} \tag{4.16}$$

where Q_n is the energy capacity of the battery, η_{mot} is the efficiency of the traction, P_{e_g} is the supplied power from engine through generator.

The charging battery operation modes include regenerative braking and battery charging from the engine. When the energy flows from the driven wheels to the battery, the motor power P_{mot} is

$$P_{mot} \cdot \eta_{mot}^{-sign(P_{mot})} - P_{e\_g} = \frac{(x(k) - x(k+1)) \cdot Q_n}{\eta_{con}} \tag{4.17}$$

where η_{mot_g} is the efficiency of the traction motor operated as generator. The power consumed by engine is

$$P_{e\_g} = P_{mot} \cdot \eta_{mot}^{-sign(P_{mot})} - (x(k) - x(k+1)) \cdot Q_n \cdot \eta_{con}^{sign((x(k)-x(k+1))} \tag{4.18}$$

With battery energy capacity Q_n and the efficiency parameters, the engine power is determined by the SOC variation at each time interval k to $k + 1$. Because in series hybrid electric drivetrain, the engine operation has one degree of freedom to choose, the StarRotor Engine nearly constant operation torque line is assumed to be the predetermined engine-generator optimal operation line curve. Therefore the fuel consumption can be only determined by the engine output power.

4.2.3 Series-Parallel EVT hybrid electric drivetrain

Unlike series or parallel hybrid electric drivetrain, in series-parallel hybrid electric drivetrain, the battery pack output power is determined by the sum of the power of traction motor and DRM electric power [43].

$$(x(k) - x(k+1)) \cdot Q_n = P_{mot} \cdot \eta_{mot}^{-sign(P_{mot})} + P_{DRM\_e} \tag{4.19}$$

where the P_{DRM_e} is the DRM electric output power.

In order to follow the torque required from driven wheels, the traction motor operates to follow the difference between the driven wheels torque demand and DRM mechanical output torque transmitted to driven wheels, therefore the power flow required from the traction motor is determined by the driven wheels power demand and the DRM mechanical output power [44][45].

$$P_{mot} = (T_{wh} - T_{DRM} \cdot R_{DRM}) \cdot \omega_{wh} \tag{4.1}$$

where T_{wh} is the torque demand from the driven wheels, T_{DRM} is the DRM mechanical torque output, R_{DRM} is the DRM gear ratio and ω_{wh} is the rotational speed demand from driven wheels.

The DRM electric power flow is used to balance the difference between the battery output power P_{bat} and the traction motor output power P_{mot}, in other words, the DRM electric power flow is determined by the battery output power P_{bat} which is also the control variable for dynamic application on series-parallel EVT hybrid electric drivetrain [46].

4.3 Summary

In this chapter, the dynamic programming is developed to find out the optimal control sequence and optimal fuel economy for the three different kinds of HEV hybrid electric drivetrains. The simulation results obtained by this application will be discussed in following chapter.

CHAPTER V

DRIVE CYCLES AND SR–HEV COMPONENTS DESIGN

For different hybrid electric drivetrain topologies, the power plant components have different design requirements and constrains. In order to meet the requirements from both of vehicle performance and drive cycles, the power plant components design analysis are discussed in this chapter. In this research, the hybrid electric drivetrain components design is based on not only the vehicle performance, which is widely used, but also the drive cycle's data, which offers more information for different hybrid electric drivetrain topologies.

5.1 The tested drive cycles

There are a number of different drive cycles in the world today. The ones presented and simulated in the thesis are Urban Dynamometer Driving Schedule (UDDS) and Highway Fuel Economy Driving Schedule (HWFET) [48].

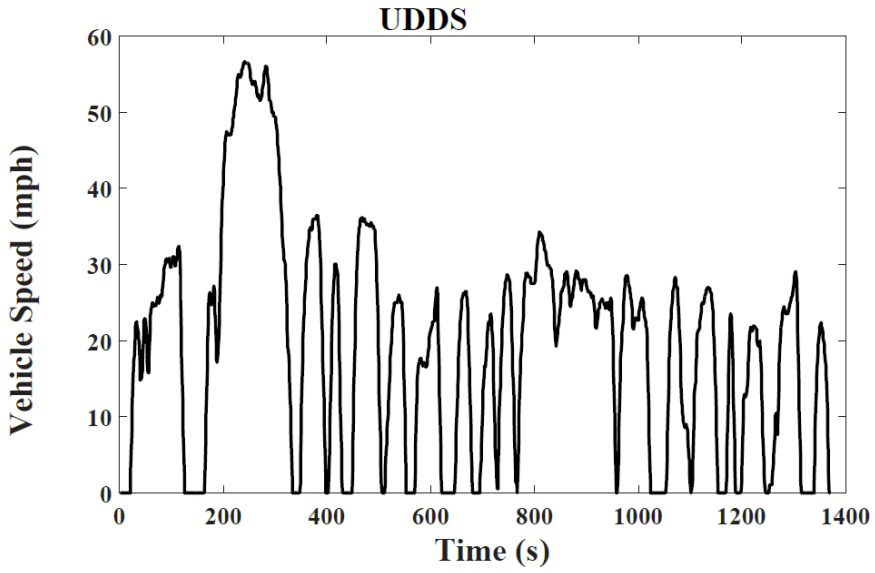

Figure 12 Vehicle speed of UDDS drive cycle.

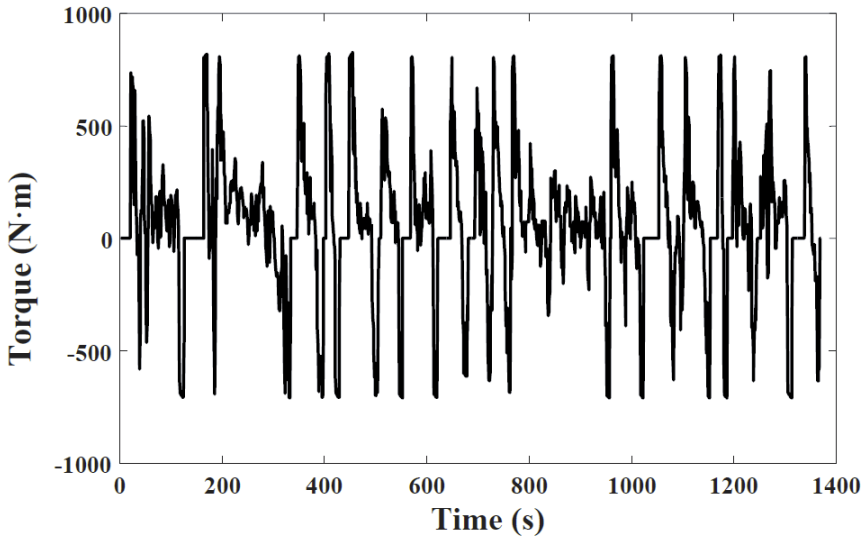

Figure 13 Driven wheels torque demand for UDDS drive cycle.

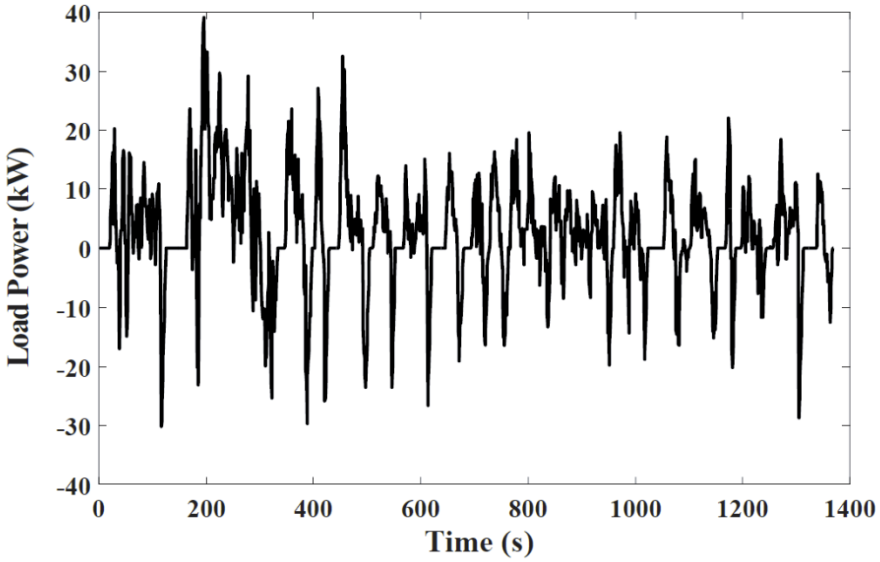

Figure 14 Driven wheels power demand for UDDS drive cycle.

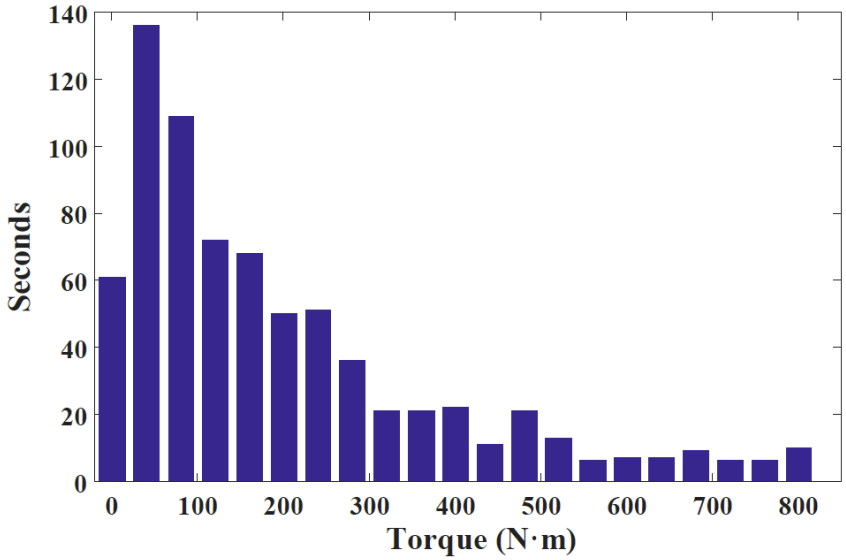

Figure 15 Torque distributions for UDDS drive cycle.

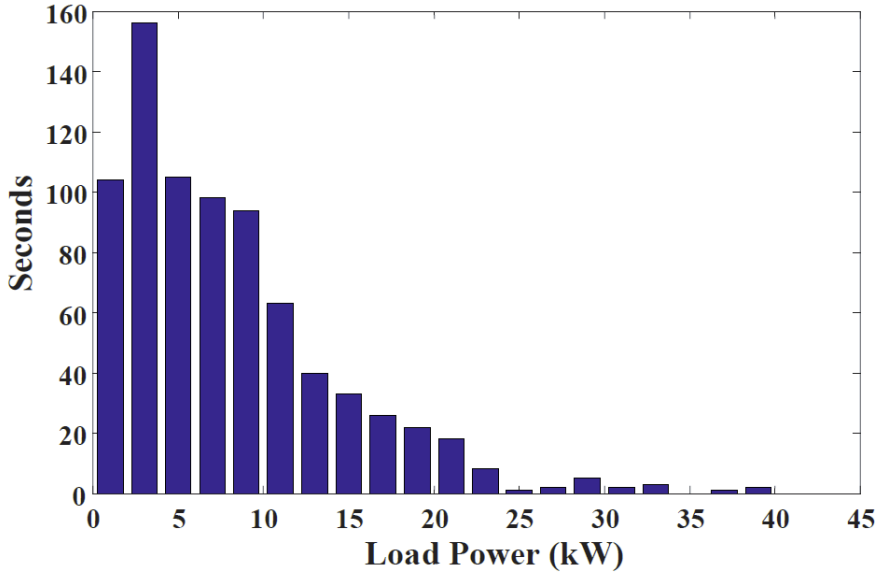

Figure 16 Load power distributions for UDDS drive cycle.

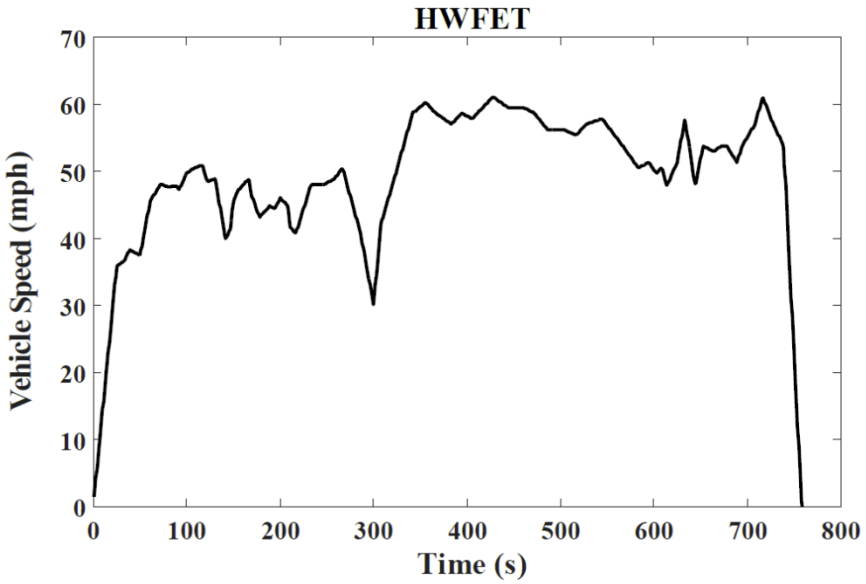

Figure 17 Vehicle speed of HWFET drive cycle.

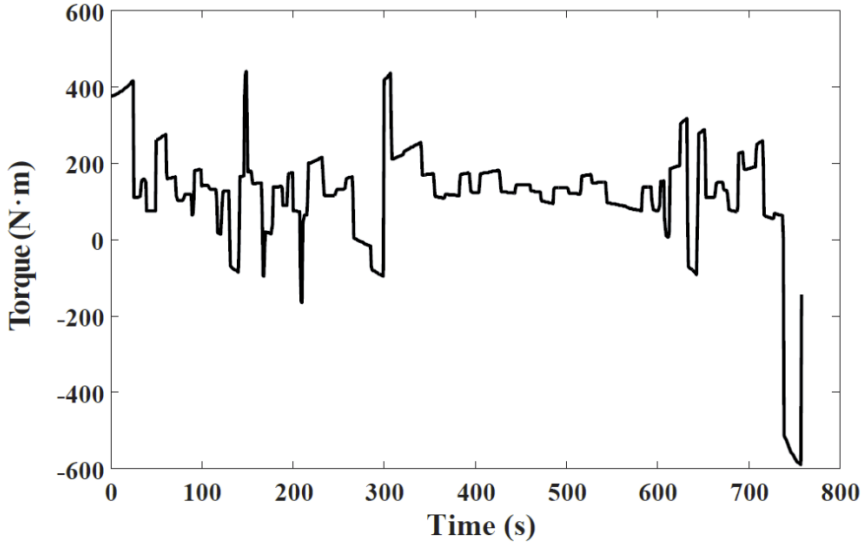

Figure 18 Driven wheels torque demand for HWFET drive cycle.

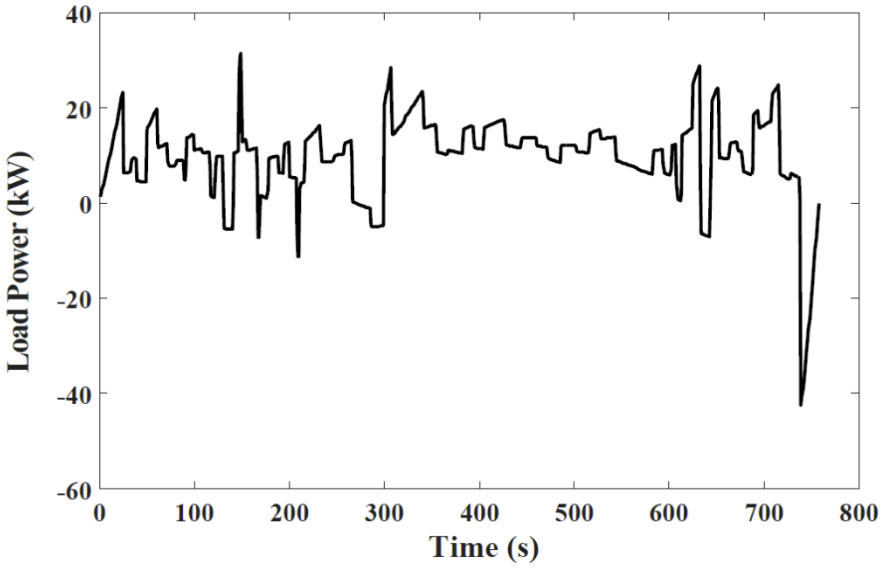

Figure 19 Driven wheels power demand for HWFET drive cycle.

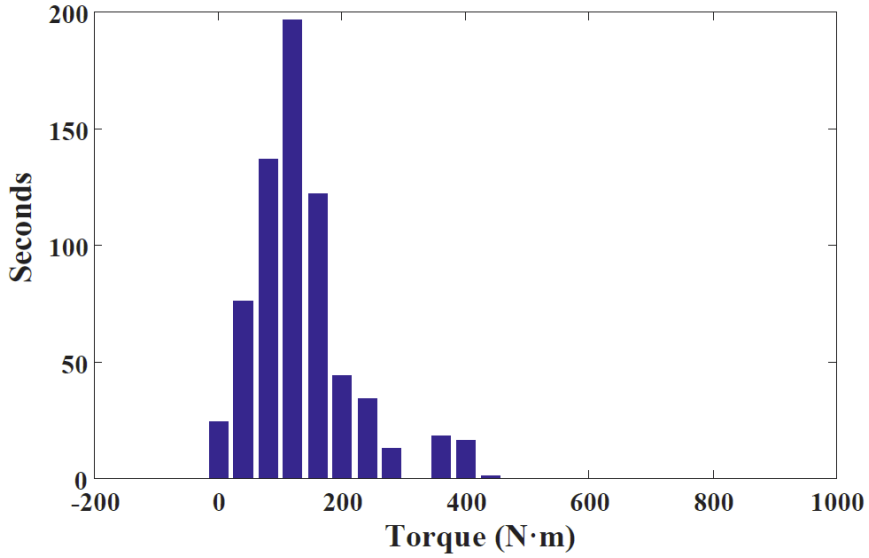

Figure 20 Torque distributions for HWFET drive cycle.

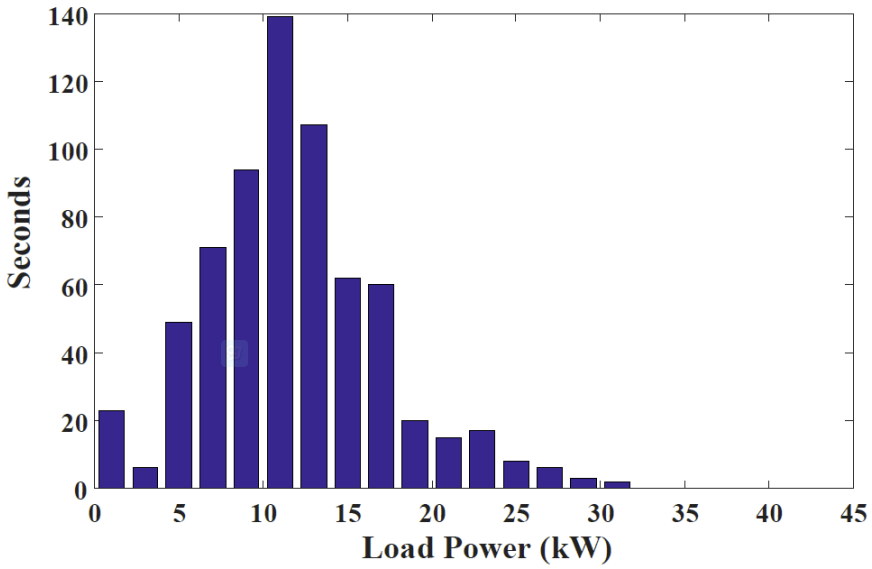

Figure 21 Load power distributions for HWFET drive cycle.

Figure 12 shows the required speed of the driven wheels during the UDDS drive cycle. The torque and power demanded from the driven wheels are shown in the Figure 13 and Figure 14 respectively. As seen in Figure 15, the maximum torque is about 800 N·m, the operation time at different torque levels in intervals of 40 N·m for torque demand. 50% of the time it operates below 120 N·m, 75% of the time below the 240 N·m and it only operates short time periods at higher torques. Figure 16 indicates that the 50% of time it operates bellows 8kW, 80% of the time below 15kW. Figure 17 through Figure 19 shows the HWFET drive cycle data which are vehicle speed, torque demand, power demand. The torque distribution and the power distribution are shown in Figure 20 and Figure 21 respectively. As seen in Figure 20, the maximum torque is about 400 N·m, the operation time at different torque levels in intervals of 40 N·m for torque demand. 60% of the time it operates below 120 N·m, 85% of the time below the 200 N·m, and it only operates short time periods at higher torques. Figure 21 indicates that the 60% of time it operates bellows 12kW, 90% of the time below 20kW. Both drive cycles data indicate the maximum torque is often a short transient and low power demand is a usual condition.

The analysis above means both drive cycles requires low power rating operation, the UDDS torque demand is higher than HWFET, and the power demand for HWFET is higher than the UDDS. Therefore control management for low power rating with high speed and low torque will determine the fuel economy.

Except the drive cycles, which will be simulated later, there are other driving conditions needed to be met by the designed vehicle as listed below: 1) Acceleration 0~60 MPH within 12 seconds; 2) Gradeability, 3% slope @ maximum speed 100mph.

For the acceleration, from 0 to 60MPH, the engine and traction motor keep operating at their maximum output torque line, and the transmission or gearbox will deliver the maximum output torque to the driven wheels [1]. The acceleration time is expressed as:

$$T_{acc} = \int_{V_1}^{V_2} \frac{M\,\delta}{\frac{T_{\text{wheel}}}{r} - M\,g\,f_r - \frac{1}{2}\rho_a C_D A_f V^2} dV \tag{5.1}$$

where the radius of driven wheels r = 0.28 m, T_{wheel} is torque transferred to the driven wheels. Besides the acceleration, the maximum vehicle speed with gradeability is the other criteria for vehicle power plant design. Gradeability is defined as the grade angle that the vehicle can overcome at a certain constant speed. In this study, the gradeability is set to 3% at 100 mph. The engine is supposed to be powerful enough to reach the maximum speed on the 3% grade road at 100 mph. Thus, according to the equation 3.1, when the vehicle speed goes up to 100 mph, the resistance power for the 3% grade road is 80 kW.

5.2 Components power rating

In this study, the vehicle design is more focused on the components power rating design. For a different hybrid electric drivetrain, the components are similar, but the

power rating makes a big difference due to different operating purposes and vehicle operation modes.

For SR–HEV, the battery pack is much more important than the conventional ICE engine based HEV because of the engine startup constrain; the battery pack has to be able to deliver enough power for the vehicle propulsion before the StarRotor Engine operates properly. The battery pack disadvantages still heavily prevent HEV and EV development. In HEV, unlike EV, the battery pack is more considered as a power source, not an energy source in EV. Therefore, the battery pack power rating is designed to be as small as possible in order to minimize the battery pack issues.

For battery power rating used in all hybrid electric drivetrains mentioned before, as shown in the Figure 5.3 and Figure 5.8, the power rating for the beginning 120 second is no more than 25 kW. The battery pack should be designed at about 25 kW. Another constraint for battery design is the hardest acceleration during the drive cycle, the power difference between the maximum engine power and the maximum power required by the drive cycle should be provided by the battery pack. As can be seen from the Figure 5.3 and Figure 5.8, the maximum power required during the drive cycle is 40 kW compared to the maximum engine power of 80 kW. The major concern for battery power rating design is beginning period battery constraint which determines a minimum required battery power of 25 kW in order to be able to meet demand from the UDDS and HWFET drive cycle.

5.2.1 Conventional drivetrain

In a conventional drivetrain, the engine, the only onboard power plant component, has to guarantee not only the vehicle at normal constant speeds on both a flat and a mild grade road but also the acceleration performance of the vehicle [1].

In the conventional drivetrain, the multi–gear is the only component to help the engine to follow the torque and speed demand from driven wheels. According to [1], for the vehicle engine power rating level, the StarRotor Engine has about 13,500 RPM for maximum rotational speed, which is much higher than the maximum rotational speed of the conventional ICE. Therefore this is necessary for the StarRotor Engine based conventional drivetrain vehicle to have a multi–gear with high gear ratio in order to converting to engine's high speed and low torque to requirements from by the driven wheels. The conventional multi–gear box mechanical efficiency is assumed at 95% each stage, the efficiency of direct gear is also assumed at 95%. In StarRotor case, such high reduction ratio cases the efficiency of multi–gear box would be 70%.

Table 5 The Multi–gear and final drive ratio

1^{st} gear	4.58
2^{nd} gear	2.96
3^{rd} gear	1.91
4^{th} gear	1.45
5^{th} gear	1.00
6^{th} gear	0.75
Final drive ratio	11.89

Because the required torque on the driven wheels depends on the wheel rotational speed and gear ratio used in the multi–gear box, the 6 gear ratios for the six-gear multi–gear box and the ratio of the final drive used in this research are listed in Table 5. The engine power rating, calculated based on the both requirements and gearbox parameter, is estimated about 120kW.

In conventional drivetrain, due to lack of second power source, the StarRotor Engine based vehicle has to wait 120 second for the engine startup. Therefore, there is impossible for this kind drivetrain to immediately to follow the drive cycle demand until the engine already reaches the specific temperature. Moreover, the StarRotor Engine nearly constant output torque can't meet the dynamic demands from driven wheels and vehicle performance requirements. Therefore the simulation can't be processed for conventional drivetrain with a StarRotor Engine.

5.2.2 Parallel hybrid electric drivetrain

A parallel hybrid electric drivetrain design is based on the conventional drivetrain mentioned above. With the same multi–gear box and final drive parameters mentioned above, the hybrid electric drivetrain has another shaft with traction motor connected to the torque coupler [49]. As same as conventional drivetrain, the power required by the vehicle at the maximum speed is completely supported by the engine. The acceleration could be benefited by this hybrid electric drivetrain for sure because the traction motor helps with the torque on the driven wheels. The acceleration performance could be estimated by equation 5.1. Unlike conventional drivetrain the T_{wheel} is not only

come from engine through multi–gear box, in parallel hybrid electric drivetrain the T_{wheel} should be calculated as follows,

$$T_{\text{wheel}} = T_{eng\_w} + T_{mot\_w} \tag{5.2}$$

where T_{eng_w} and T_{mot_w} are engine torque and electric motor torque transmitted to the driven wheels through the gearboxs, respectively.

The traction motor with well control could keep maximum torque while its speed goes up to the base speed with constant flux. Beyond the base speed, the flux is weakened which results in a constant output power while the torque decreases hyperbolically with its speed. Due to the characteristics of the StarRotor Engine the traction motor has to propel the vehicle alone until the StarRotor Engine gets operational temperature. Therefore the traction motor has to be designed for enough power to track the demand from driven wheels during the beginning period. Based on the same idea of battery pack design, as shown in the Figure 5.5 and Figure 5.10, the power rating for the beginning 120 second is no more than 25 kW, the traction motor is reasonable to be designed as 25 kW. However except the beginning 120 second, the traction is also required in acceleration performance. Based on the engine power rating design mentioned in section 5.1, the 80 kW engine alone is impossible to meet the acceleration performance request. Therefore the traction motor power rating is necessary to be increased to 30 kW.

The battery is the only energy and power resource to the traction motor, therefore the battery has both energy and power requirement. In this study, the energy/power ratio

of the battery is 0.3h In order to supply enough power to this 30 kW traction motor case, the Lithium-Ion battery pack should have 7 kWh on board.

5.2.3 Series hybrid electric drivetrain

The series hybrid electric drivetrain design is totally different from parallel, all vehicle performances are depended on the traction motor, the only propel component in this hybrid electric drivetrain, which has to be designed powerful enough to track the driven wheels demands [49]. The power rating of the traction motor can be estimated, according to [1], the acceleration performance could be estimated,

$$P_{mot} = \frac{\delta M}{2T_{\text{acc}}}(V_f^{\,2} + V_b^{\,2}) + \frac{2}{3}Mgf_r V_f + \frac{1}{5}\rho_a C_D A_f V_f^{\,3} \tag{5.3}$$

where the P_{mot} is the power rating of the traction motor, V_b is the vehicle speed corresponding to the traction motor base speed, V_f is the final speed during the acceleration. The P_{mot} compares with the power for maximum speed with 3% gradeability, the bigger one would be the estimated power rating for the series hybrid electric drivetrain traction motor.

The idea of the series hybrid electric drivetrain is to keep engine to work along the optimal operation line which is the operation line where the engine operates at optimal efficiency for a required power while meet the driven wheels demand at final gear. At the same time the other vehicle components should also work cooperatively in order to maximize the system efficiency or minimize the fuel consumption.

In this hybrid electric drivetrain the StarRotor Engine connects to a generator, these two components are used to generate electric power in order to prevent the battery

from being discharged completely. In the design process, the power for the constant speed driving at maximum speed is needed to be considered. As mentioned before driving at the 100 mph with 3% grade requires 80 kW for the traction motor output power rating. The engine should be able to provide sufficient power to support the traction motor requirement at vehicle maximum speed with the losses during the energy conversion. Therefore the StarRotor Engine is supposed to design at 105 kW.

As mentioned in parallel hybrid electric drivetrain, the battery pack is required due to the engine characteristics, the battery is the only energy and power resource to the traction motor until the engine fully operates, therefore the Lithium-Ion battery pack should have 8 kWh on board in order to provide enough power to the traction motor.

5.2.4 Series-Parallel hybrid electric drivetrain

The design of series-parallel hybrid electric drivetrain is similar to the series hybrid electric drivetrain but more complicated because engine is not only linked to the DRM but also to driven wheels [51].

Because the engine and DRM have different maximum rotational speeds, there is an engine single–gear box required between engine and DRM in order to avoid over-speed situation happened on the smaller one side. The same philosophy can be applied to the traction motor single–gear box and DRM single–gear box as well.

The easiest way to determine the value of these gear ratios is to set the ratio value as same ratio between the maximum rotational speeds on both side. In fact, the gear ratios could be designed in a wide range, for example, the maximum DRM gear ratio could be the ratio between the DRM maximum rotational speed and driven wheels

rotational speed at maximum designed vehicle speed in which case the vehicle design is more like parallel hybrid electric drivetrain because the driven wheels takes engine torque as much as possible. The minimal DRM gear ratio could be the ratio between the base rotational speed of DRM and the driven wheels rotational speed at maximum vehicle designed speed in which case the vehicle design is more like series hybrid electric drivetrain because the torque of driven wheels comes more from the traction motor. The DRM gear ratio not only affects the torque distribution at vehicle maximum speed but also affect the vehicle fuel economy as well. The sensitivity of gear ratios will be analyzed in Chapter VII.

5.3 Design procedure of the hybrid electric drivetrain components

In this study, it is assumed that for engine and electric machine the torque and losses are supposed to be proportional to the power, thus while the torque, losses and weight could be multiplied by power ratio factors but efficiency maps pattern remains the same, which seems a reasonable assumption as long as the machines and engine remain in an small interval.

All hybrid electric drivetrain design mentioned above is initial estimation based on the requirements on the vehicle e.g. acceleration, top speed and so on. The required the power and torque demand from driven wheels can be used to specify the hybrid electric drivetrain components power rating based on the hybrid electric drivetrain characteristics. As mentioned before, for engine and electric machines, as long as they are in a reasonable interval of power rating the efficiency maps pattern remains the same

as the torque and losses shares the same factor. Therefore the component weights are supposed to be proportional to their power ratings and multiplied the same factors. The battery pack weight is simply proportional to the power rating or the energy.

After updating the vehicle weight based on the components estimated weights, the updated vehicle with estimated components would be tested for the vehicle performance requirements again. If the updated vehicle meets the requirements then the whole drive cycle would be simulated in next step, otherwise, the components needs to be estimated again based on the updated vehicle information. After passing the performance testing, the updated vehicle also needs to be tested in specific driving cycles in order to make sure the battery size and traction motor are designed powerful enough to propel the vehicle alone until the StarRotor Engine can operate properly. The Figure 22 shows an iterative step by step procedure for designing and estimating the vehicle with power plant components.

5.4 Summary

Except vehicle performances, the drive cycle data are also taken account into the vehicle onboard power plant components design. Because of StarRotor Engine's startup feature and the limited battery pack power rating and energy performance, in this study, the battery power rating is designed as low as possible in order to fully utilize StarRotor Engine. The other components have their different requirements for different hybrid electric drivetrain.

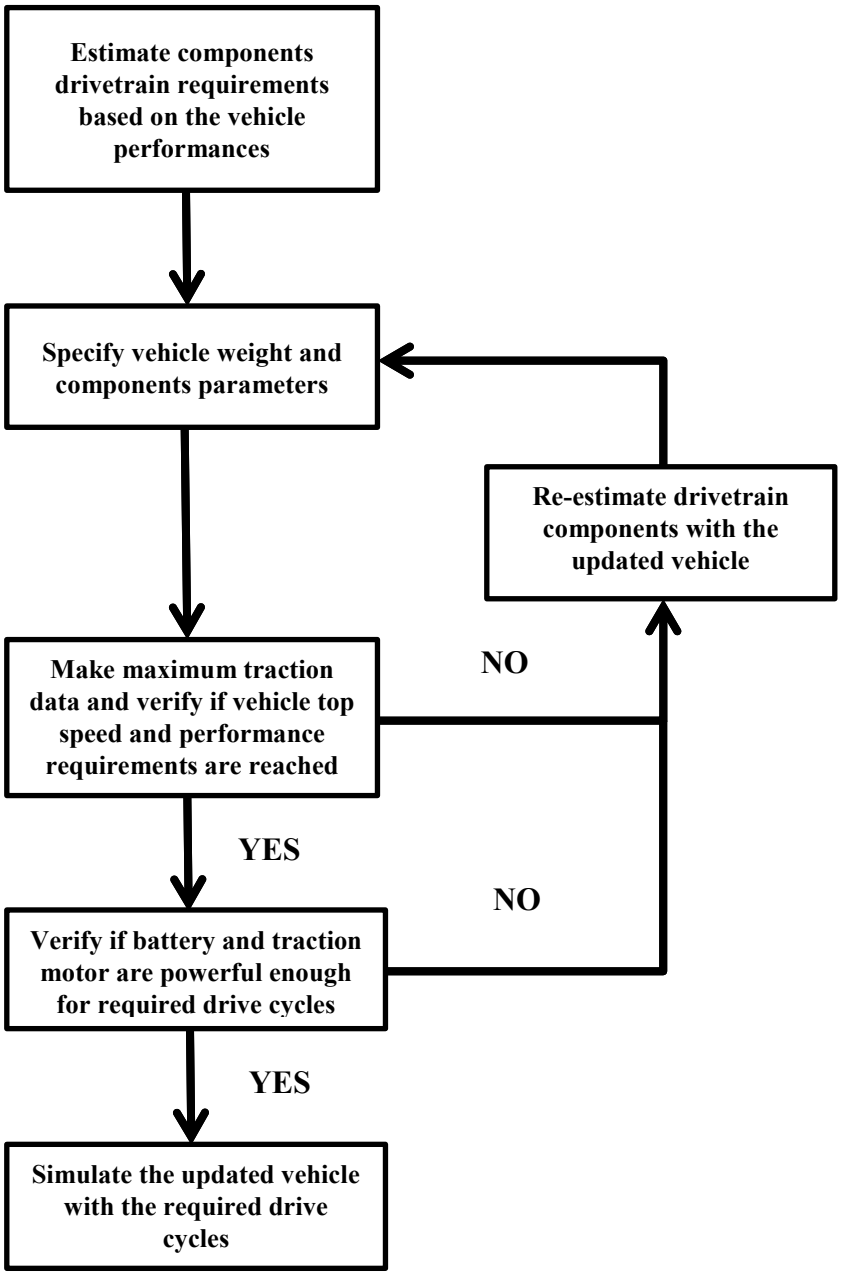

Figure 22 Schematic of the design procedure.

CHAPTER VI

SIMULATION RESULTS AND COMPARISON

Based on onboard power plant components discussed in Chapter V and control strategy mentioned in Chapter IV, the vehicle fuel economy can be simulated by the dynamic programming in Matlab. The fuel economy for each hybrid electric drivetrain on a typical driving cycle can be calculated. In order to determine the best fuel economy hybrid electric drivetrain for SR–HEVs, the optimal fuel economy of each hybrid electric drivetrain will be compared.

6.1 Parallel hybrid electric drivetrain

A brief summary of this parallel hybrid electric drivetrain is presented in Table 6. The dynamic programming is used to simulate the control strategy for the parallel hybrid electric drivetrain with the detailed component information. The StarRotor Engine operation points during UDDS are shown in Figure 23. The traction motor operation points are shown in Figure 24，and the battery SOC variation is shown in Figure 25. The fuel economy for UUDS drive cycle achieved is 69.45 MPG.

Table 6 Summary of the parallel HEV

Engine	Traction motor	Battery	Vehicle mass
80 kW	30 kW	7 kWh	1630 kg

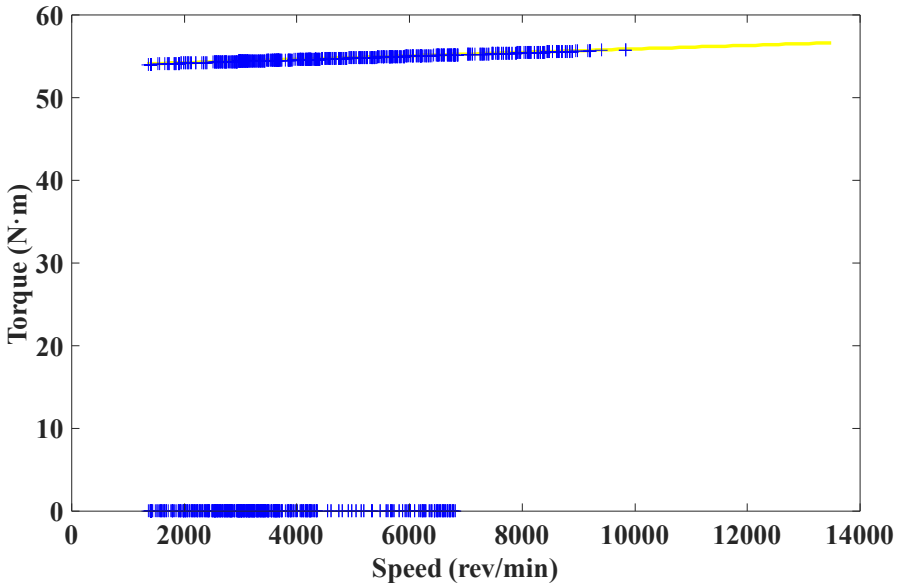

Figure 23 Engine operation points for the StarRotor Engine based parallel HEV during UDDS drive cycle.

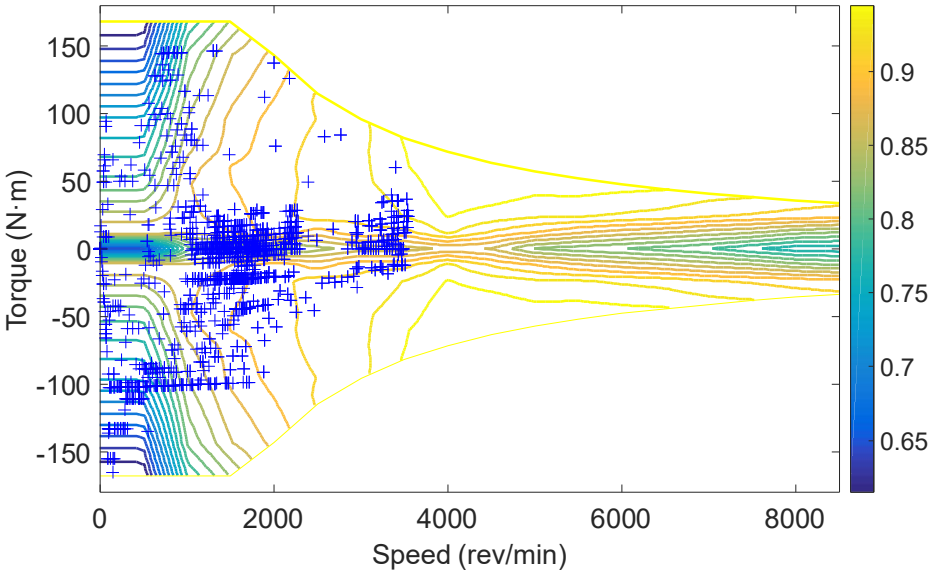

Figure 24 Traction motor operation points for the StarRotor Engine based parallel HEV during UDDS drive cycle.

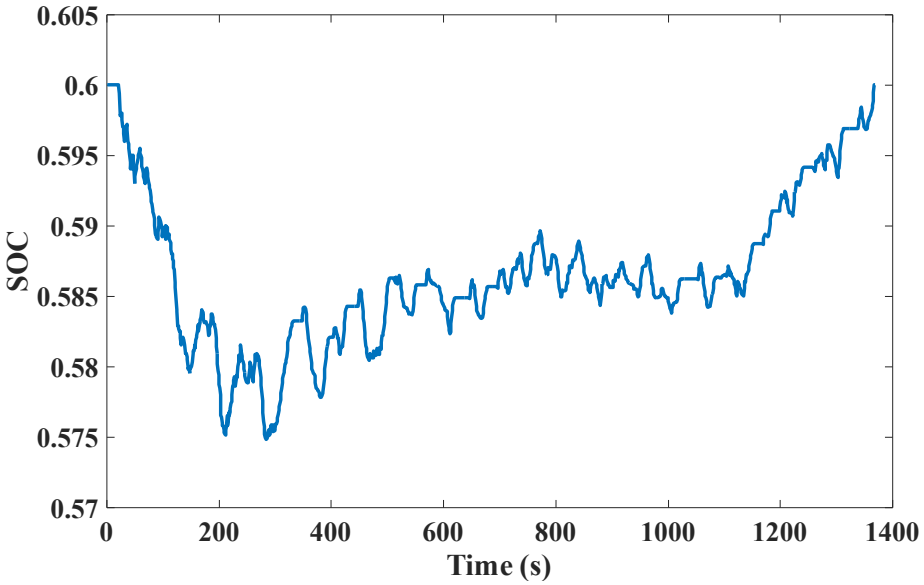

Figure 25 SOC variation for the StarRotor Engine based parallel HEV during UDDS drive cycle.

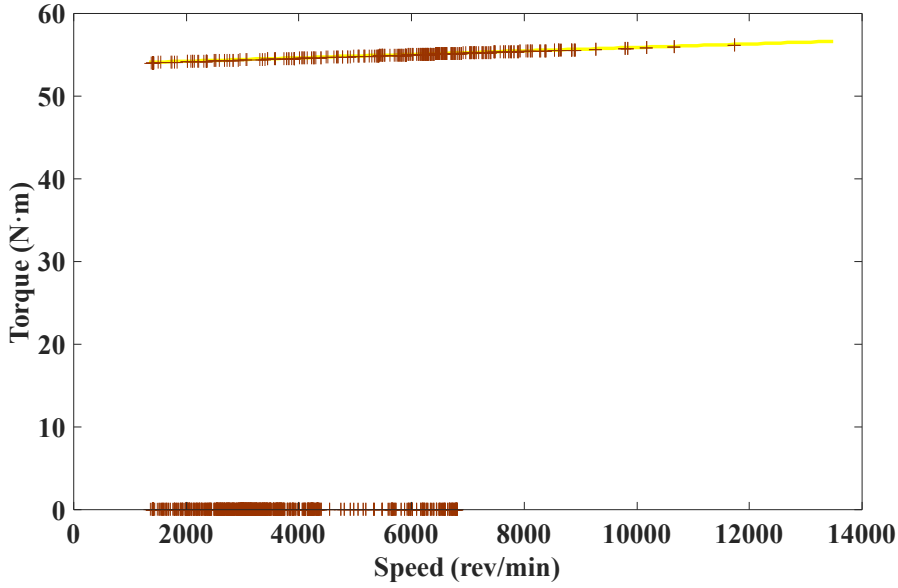

Figure 26 Engine operation points for the StarRotor Engine based parallel HEV during HWFET drive cycle.

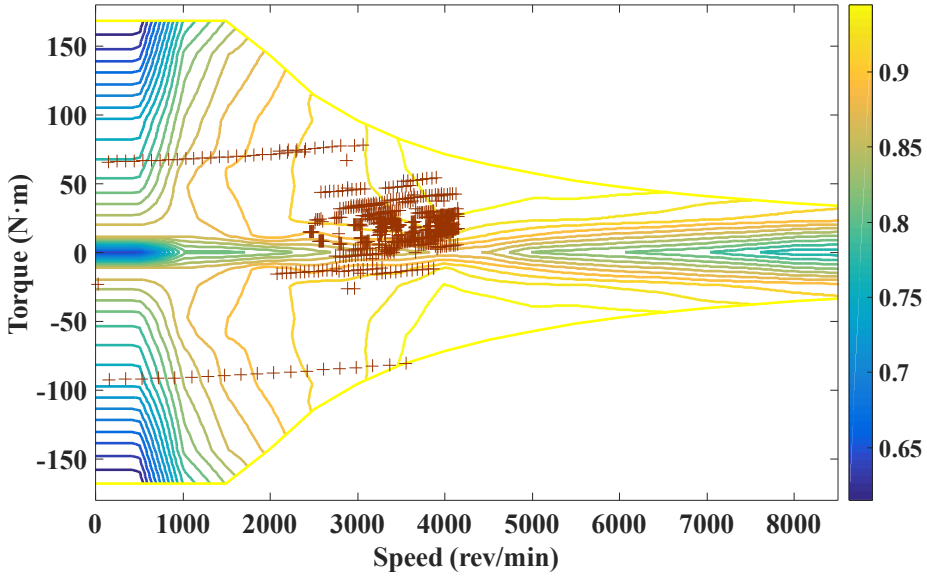

Figure 27 Traction motor operation points for the StarRotor Engine based parallel HEV during HWFET drive cycle.

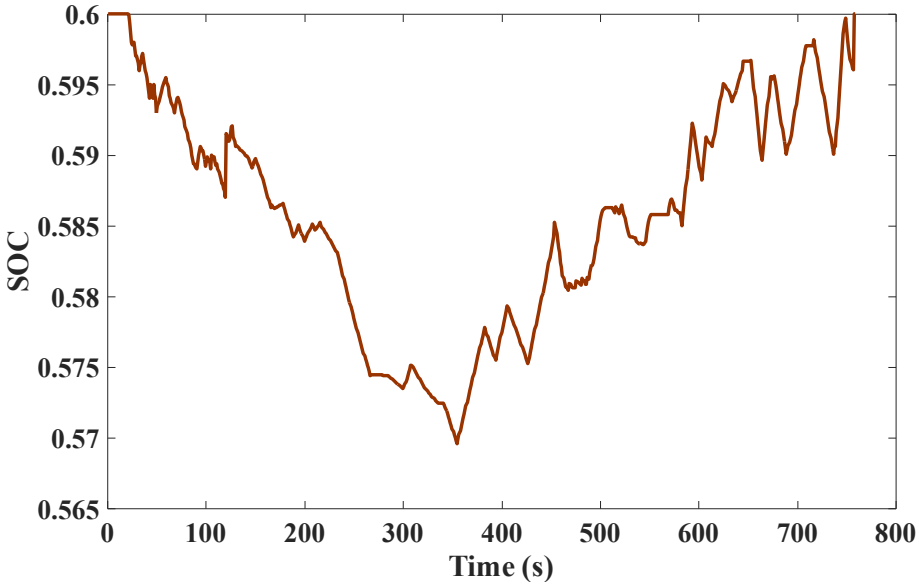

Figure 28 SOC variation for the StarRotor Engine based parallel HEV during HWFET drive cycle.

The HWFET is the other important driving cycle to simulate. The engine and traction motor operation points are shown in Figure 26and Figure 27 respectively. The SOC variation is shown in Figure 28. According to the simulation, the optimal fuel economy for the HWFET drive cycle is 79.86 MPG.

6.2 Series hybrid electric drivetrain

The components summary for a series hybrid electric drivetrain is shown in Table 7 as mentioned in Chapter V for the series hybrid electric drivetrain design. the dynamic programming simulation results of engine and traction motor operation points for UDDS drive cycles are shown in Figure 29 and Figure 30 respectively. The SOC variation of this drive cycle is shown in Figure 31. For the HWFET drive cycle, the engine and traction motor operation points are shown in Figure 32 and Figure 33 respectively. The SOC variation for HWFET drive cycle is shown in Figure 34.

Table 7 Summary of the series HEV

Engine	Traction motor	Generator	Battery	Vehicle mass
105 kW	95 kW	85 kW	8 kWh	1780 kg

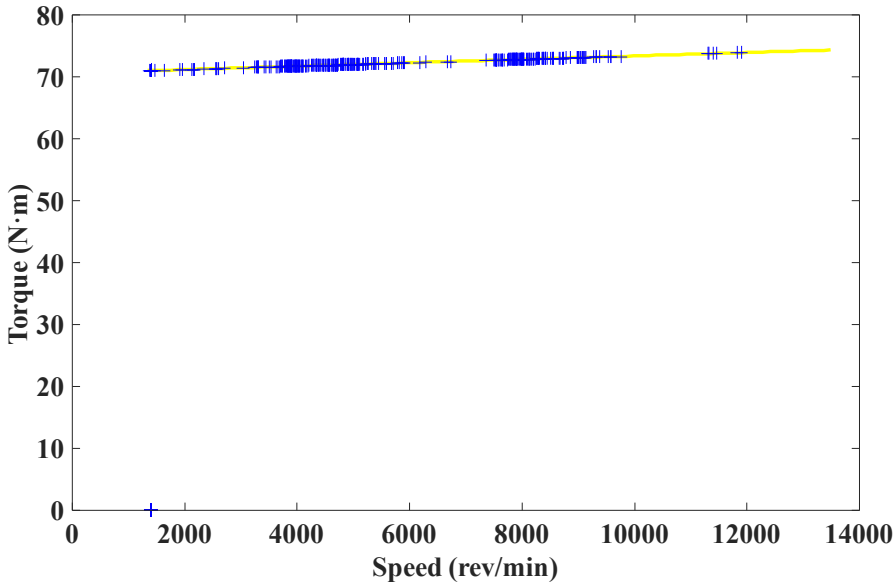

Figure 29 Engine operation points for the StarRotor Engine based series HEV during UDDS drive cycle.

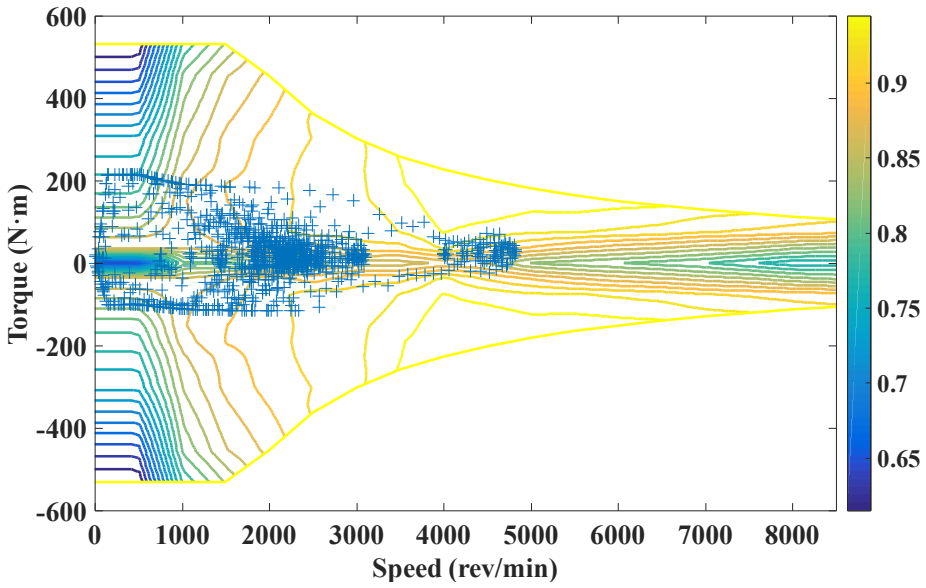

Figure 30 Traction motor operation points for the StarRotor Engine based series HEV during UDDS drive cycle.

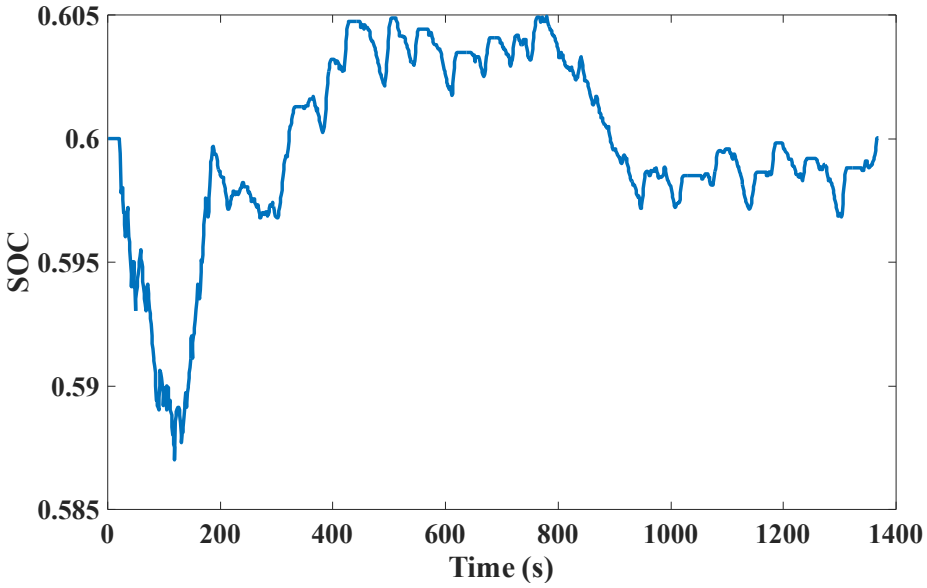

Figure 31 SOC variation for the StarRotor Engine based series HEV during UDDS drive cycle.

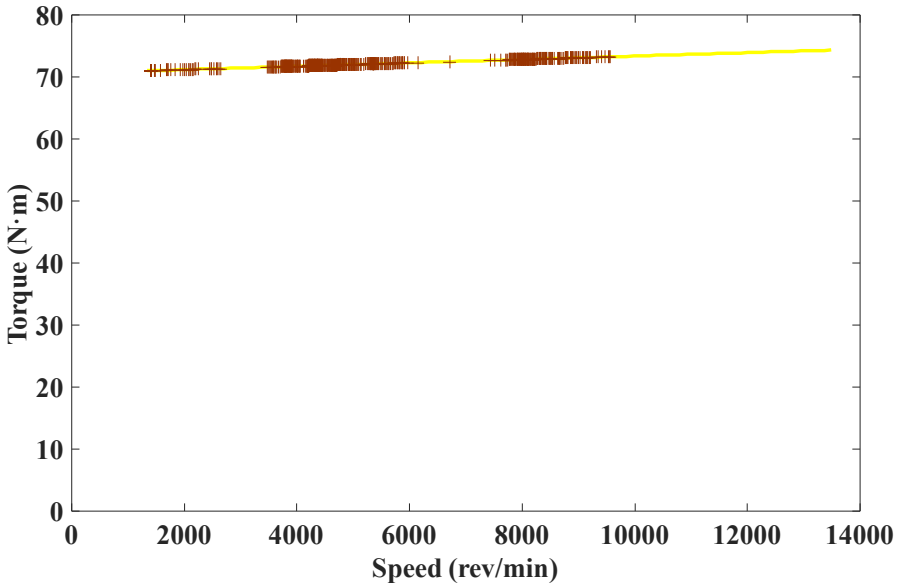

Figure 32 Engine operation points for the StarRotor Engine based series HEV during HWFET drive cycle.

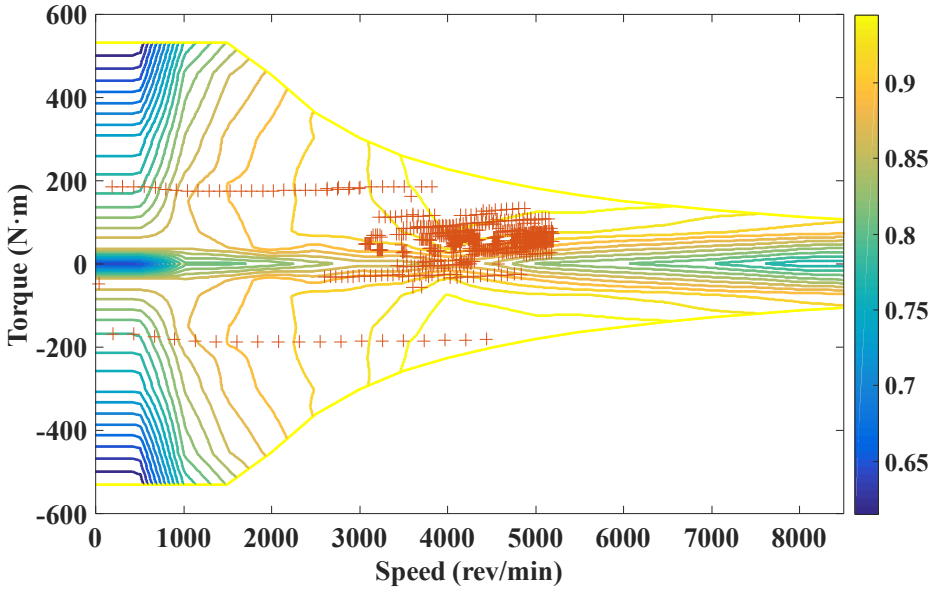

Figure 33 Traction motor operation points for the StarRotor Engine based series HEV during HWFET drive cycle.

.

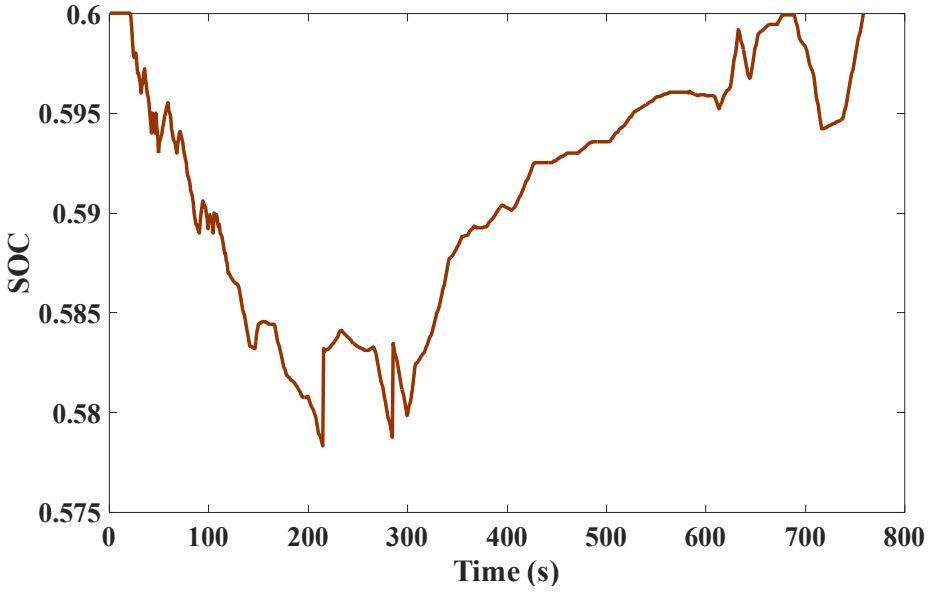

Figure 34 SOC variation for the StarRotor Engine based series HEV during HWFET drive cycle.

For this series hybrid electric drivetrain, the fuel economy of both drive cycles are 75.42 and 84.45 respectively. Compared with the parallel hybrid electric drivetrain, the MPGs of the series hybrid electric drivetrain are marginally higher because of the series hybrid electric drivetrain multiple times of energy transformation and additional weight from drivetrain components.

6.3 Series-parallel hybrid electric drivetrain

Table 8 shows the summary of the components of the series-parallel hybrid electric drivetrain. The dynamic program applied to the series-parallel hybrid electric drivetrain model shows the engine operation points during the UDDS and HWFET drive cycles in Figure 35 and Figure 38 respectively. The traction motor operates to assist the engine in following the driven wheels torque demand as shown in Figure 36 and Figure 39. The fuel economy summary of both drive cycles are 80.77 MPG and 87.31 MPG.

Table 8 Summary of the series-parallel EVT HEV

Engine	Traction motor	DRM	Battery	Vehicle mass
85 kW	50 kW	80 kW	8 kWh	1720 kg

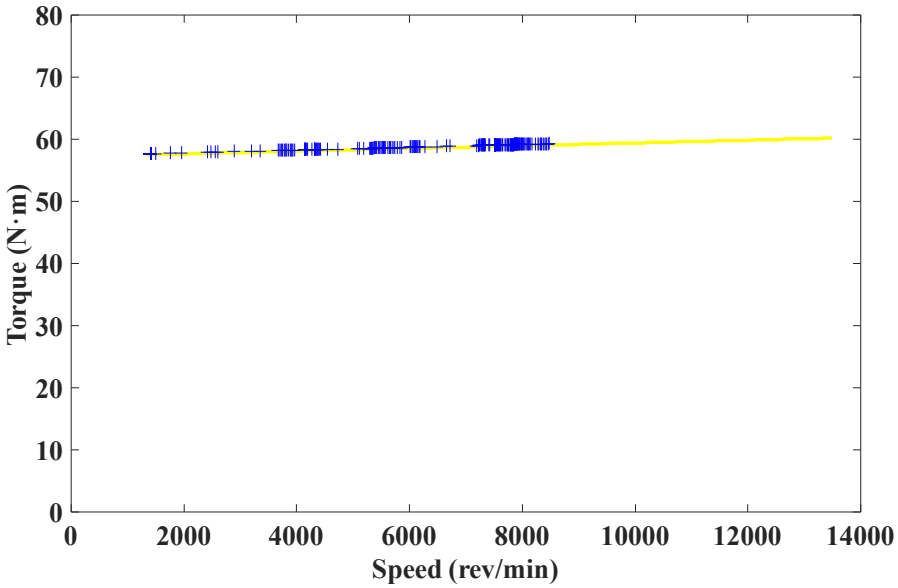

Figure 35 Engine operation points for the StarRotor Engine based series–parallel EVT HEV during UDDS drive cycle.

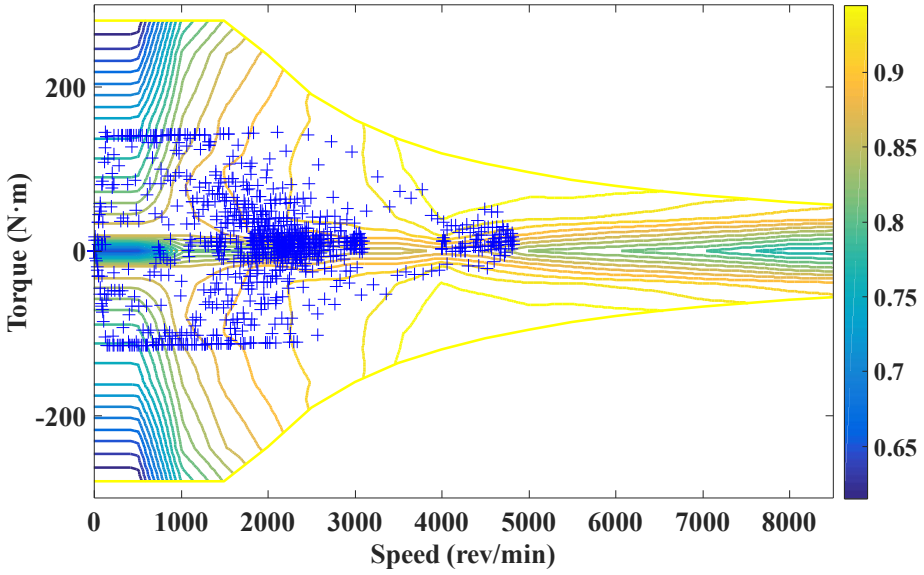

Figure 36 Traction motor operation points for the StarRotor Engine based series–parallel EVT HEV during UDDS drive cycle.

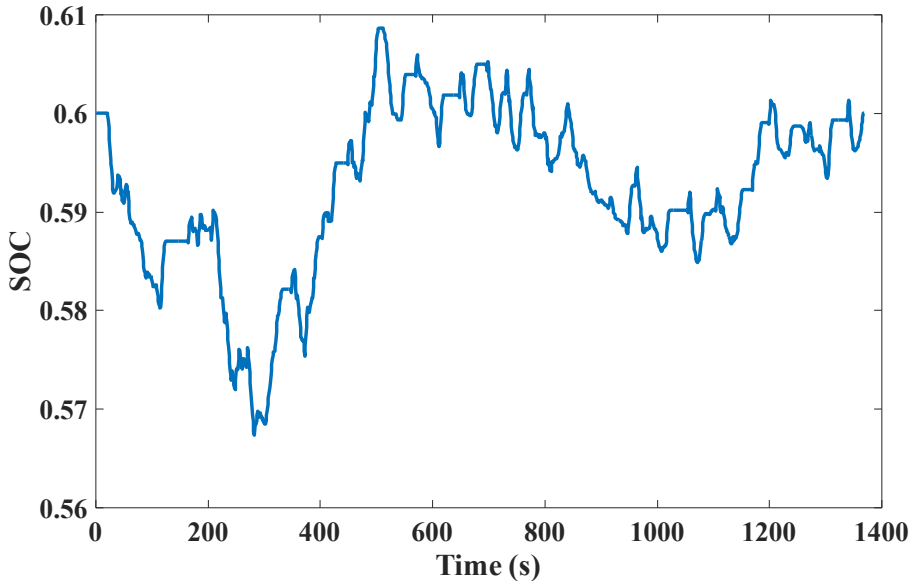

Figure 37 SOC variation for the StarRotor Engine based series–parallel HEV during UDDS drive cycle.

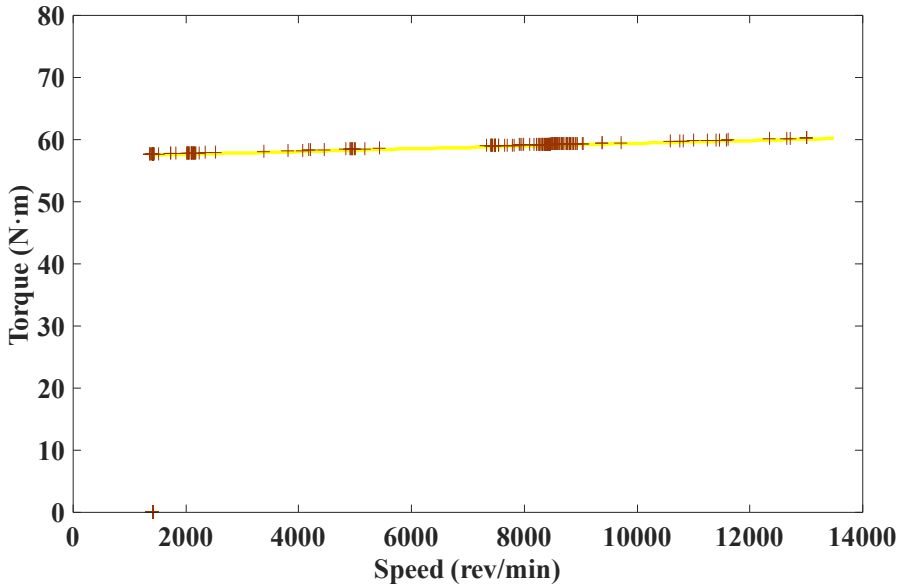

Figure 38 Engine operation points for the StarRotor Engine based series–parallel EVT HEV during HWFET drive cycle.

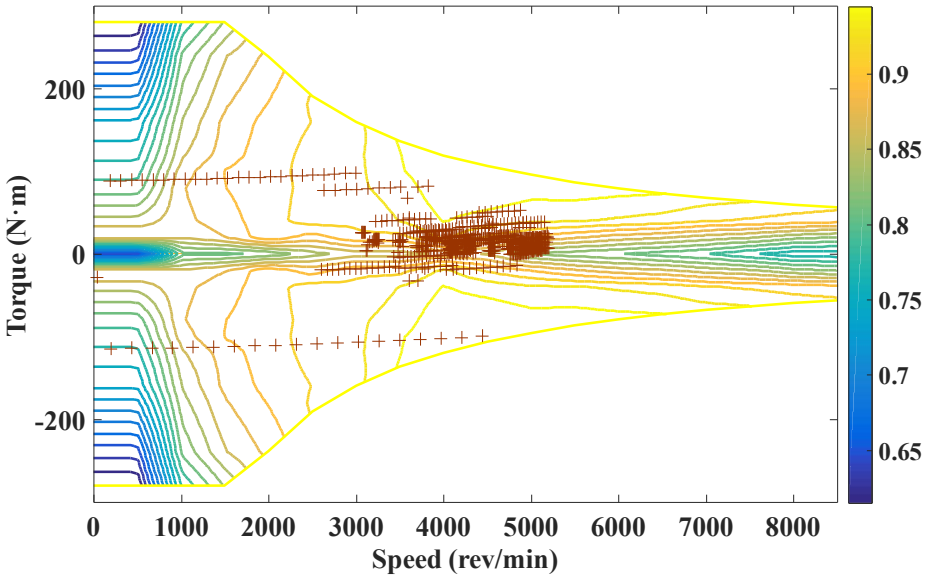

Figure 39 Traction motor operation points for the StarRotor Engine based series–parallel EVT HEV during HWFET drive cycle.

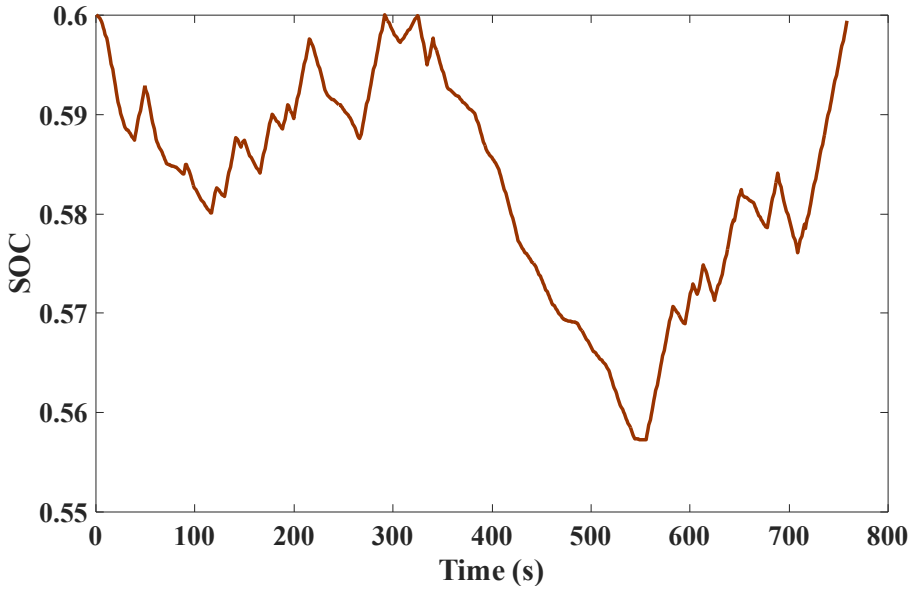

Figure 40 SOC variation for the StarRotor Engine based series–parallel EVT HEV during HWFET drive cycle.

6.4 Simulation results comparison

The simulation results indicate that the hybrid electric drivetrain can significantly improve the fuel economy of the StarRotor Engine based vehicle.

Using the same design process and simulation method, the conventional ICE based HEVs with different hybrid electric drivetrains are also simulated. The fuel economy simulation results are shown in Table 9. Compared with SR–HEV, the conventional ICE based HEVs have a much lower fuel economy because of the small efficient operation area of the conventional ICE.

Besides the HWFET and UDDS drive cycles, the IM240 and SC03 drive cycles are also simulated by the same vehicles designed for both the StarRotor Engine and conventional ICE. Figure 41 shows the comparison of fuel economy between different drive cycles for the conventional ICE engine based drivetrains, and Figure 42 shows the one for the StarRotor Engine based drivetrains. Based on the data collected, the series-parallel hybrid electric drivetrain has the best fuel economy of these three hybrid electric drivetrains with the help of the EVT.

Table 9 Fuel economy on different cycles for conventional ICE based HEVs

	UDDS [MPG]	HWFET [MPG]	IM240 [MPG]	SC03 [MPG]
Conventional	22.73	28.64	24.33	23.06
Parallel	38.67	47.62	42.15	38.05
Series	42.09	48.79	45.93	42.77
Series-Parallel EVT	55.98	58.41	49.53	52.47

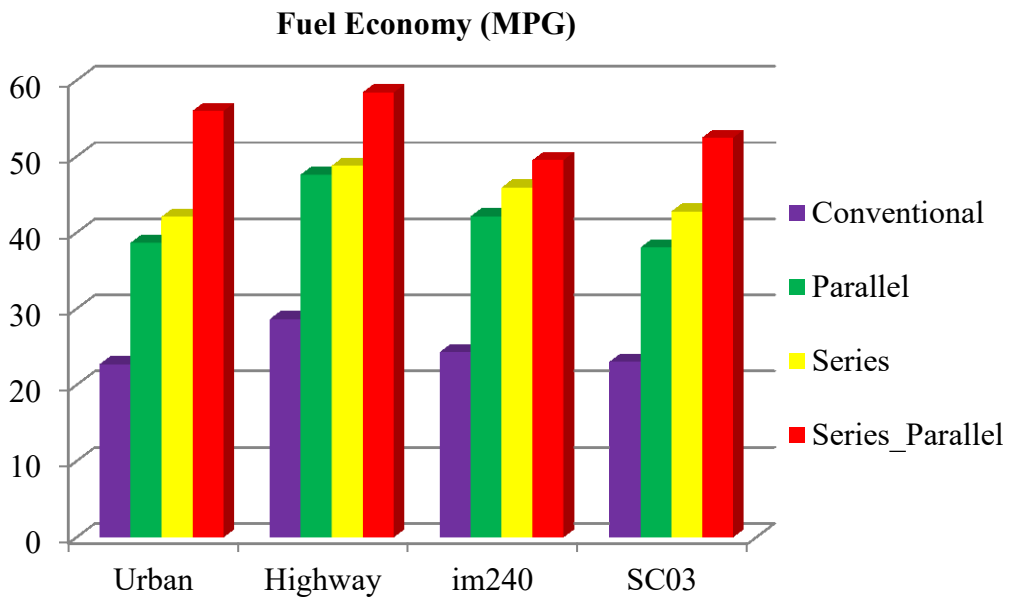

Figure 41 Fuel economy comparison of the conventional ICE based drivetrain for the different drive cycles.

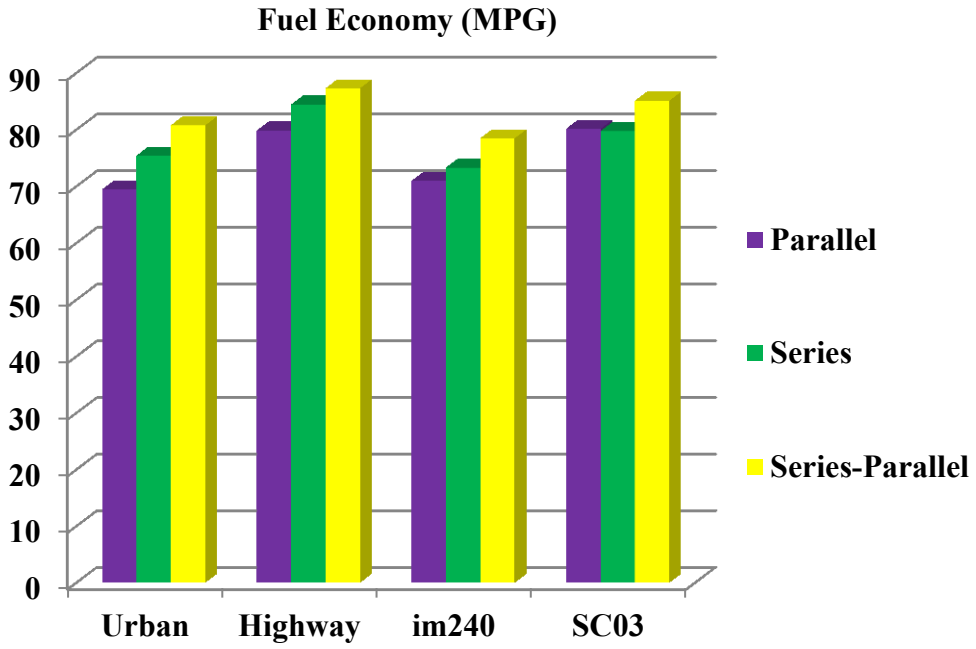

Figure 42 Fuel economy comparison of the StarRotor Engine based drivetrain for the different drive cycles.

The simulation also indicates that the fuel economy of the StarRotor Engine based parallel HEV is very similar to the series drivetrain, which means the StarRotor Engine based parallel HEV could be a promising product due to the high fuel economy improvement because of the less additional investment.

6.5 Summary

The drive cycle simulations give data on the behavior and fuel economy of these three HEV hybrid electric drivetrains. The simulation results indicate that the StarRotor Engine based vehicle provide a much better fuel economy than the conventional ICE. The hybrid electric drivetrain is very important for the StarRotor Engine based vehicle.

The comparison also indicates that the seires-parallel hybrid electric drivetrain provides the most fuel economy improvement of these three hybrid electric drivetrains.

CHAPTER VII

VEHICLE FUEL ECONOMY IMPROVEMENT FOR SERIES–PARALLEL EVT HYBRID ELECTRIC DRIVETRAIN

This chapter analyzes the sensitivity of the gear ratio parameter to a series-parallel EVT hybrid electric drivetrain to further improve vehicle fuel economy, which will provide a helpful guidance for series-parallel EVT hybrid electric drivetrain gear ratio design.

7.1 Background

Due to the unmatched speed-torque profile of any kind of engine to the required speed-torque profile on driven wheels, the gearbox is very important for all kinds of vehicles.

For the StarRotor Engine based vehicle, the gearbox is extremely crucial due to the maximum rotational speed. As mentioned in last chapter, in a series-parallel EVT hybrid electric drivetrain, unlike parallel or series hybrid electric drivetrain, the series-parallel EVT hybrid electric drivetrain has, mechanical and electric power flows provided to the driven wheels, thus power required for the maximum vehicle speed can be divided into two parts, one is mechanical power flow from DRM and the other one is from traction motor which consumed electric power flow from DRM. Both of mechanical and electric power flows come originally from the StarRotor Engine.

In Chapter V, the series-parallel EVT hybrid electric drivetrain is designed as the pure mechanical power flow, which means there is no torque assistant from traction motor while the vehicle is driven at maximum speed. Because this hybrid electric drivetrain provides an opportunity to manage the power flow distribution on driven wheels at the maximum speed of the vehicle by changing the gear ratios, in this chapter, the sensitivity of gear ratios to series-parallel EVT drivetrain for fuel economy will be further discussed.

If the DRM gear ratio decreases, the torque from DRM delivered to the driven wheels is lower than driven wheels demand at the maximum vehicle speed, and the maximum rotational speed of DRM through the DRM gear will extend the required rotational speed at maximum vehicle speed. Therefore, except for delivery of the mechanical torque from DRM directly to driven wheels, the DRM will also need to operate as generator to provide electric power to the traction motor which at the same time operates as torque assistance to balance the torque difference between required torque at maximum vehicle speed transmitted to DRM and DRM output torque through the motor gear. In this case, the driven wheels receive torque from both DRM and traction motor while the vehicle is driven at maximum vehicle speed, and all the power is only provided by the StarRotor Engine simultaneously.

The power distribution at maximum vehicle speed can be also changed if the engine gear ratio is increased. By increasing the engine gear ratio, the DRM output torque transmitted to driven wheels is higher than the required torque from the driven wheels at maximum vehicle speed; therefore, the traction motor works as generator to

provide power back to DC bus. At the same time the DRM operates traction motor to increase vehicle the speed to maximum speed.

Because all the power distribution assumption mentioned above is based on the premise that the traction motor has the ability to contribute at the vehicle maximum speed, the motor gear is unchanged. Therefore, in this chapter, the sensitivity of the engine and DRM gear ratios to vehicle fuel economy performance to an optimized series-parallel EVT hybrid electric drivetrain has been performed by applying dynamic programming method, which is reviewed in Chapter IV. The dynamic programming algorithm is implemented for both HWFET and UDDS driving cycles, which are typical ones for highway and urban driving analysis, to investigate fuel economy variation by changing power distribution.

7.2 Power distribution variations with different gear ratios

As mentioned before, the low DRM gear ratio will reduce the torque effort from DRM on the driven wheels. Thus, the low DRM gear ratio results in a similar design process for whole onboard power plant components to the series hybrid electric drivetrain design. The traction motor power rating has to be increased in order to maintain the same acceleration performance. Because the motor gear ratio is unchanged and the excellent speed-torque characteristic of traction motor, which has a much better torque performance at low speed than StarRotor Engine at the same power rating level. The percentage variation of traction motor power rating is small. The less DRM gear ratio, the DRM operates more like a series hybrid electric drivetrain with little

mechanical output power flow but provide enough electric power to the DC bus. The minimal DRM gear ratio value is the base speed of DRM divided by the maximal rotational speed of driven wheels at maximal vehicle speed.

From the equation 3.20 and 3.22, both an engine gear ratio and a DRM gear ratio can be used to change the engine mechanical torque effort on driven wheels because their product is a total gear ratio for the engine out torque. However the engine gear has one more capability, which is to manage the DRM operation torque range because the DRM operation torque is determined by the engine gear ratio and the engine output torque. In summary, the engine gear could be used to control DRM operation torque, and the DRM gear ratio is used to manipulate the engine mechanical torque effort on driven wheels.

By increasing engine gear ratio from the minimal value to the maximum value, the DRM torque is also increased. The maximum operation speed of DRM is decreased hyperbolically with its torque.

By increasing engine mechanical torque effort on driven wheels, the operation of the whole hybrid electric drivetrain is like a parallel hybrid electric drivetrain but in a different way in which the DRM provides too much torque and traction motor. And DRM has to operate as generator and traction motor respectively to track the torque and speed demand from driven wheels.

In an acceleration performance test, the traction motor does not need to operate as generator to balance the torque output from DRM, and then the both of traction motor

and DRM can provide traction torque to the driven wheels to significantly improve the acceleration performance, which is much better than the low DRM gear ratio situation.

The engine and DRM gear ratios not only separately control the DRM operation torque and speed but also manage the torque distribution for DRM and traction motor. For low engine and DRM gear ratio, the DRM torque effort on driven wheels becomes low. If the DRM output torque transmitted to driven wheels is less than most driven wheel demand. In order to follow the drive cycle flawlessly, the traction motor has to powerful enough or maybe oversized, to provide more torque support to driven wheels, in which case, the fuel economy will drop due to the energy conversion. The same situation happens when the high engine and DRM gear ratios are applied. When the DRM torque transmitted to driven wheels is larger than most demand, the traction motor either works alone or operates as generator the balance the DRM output torque effort on driven wheels. Therefore the appropriate engine and DRM gear ratios can not only minimize the energy conversion but also have the DRM and traction motor operating under efficient area.

7.3 Simulation results

The Figure 43 shows the engine gear ratio and DRM gear ratio effort on fuel economy for UDDS drive cycle. The optimal engine gear ratio R_{eng} and DRM gear ratio R_{DRM} are 2.08 and 2.66, respectively. By changing the ratios away from this point, the fuel economy decreases. The same gear sensitivities for HEFET is shown in Figure 44.

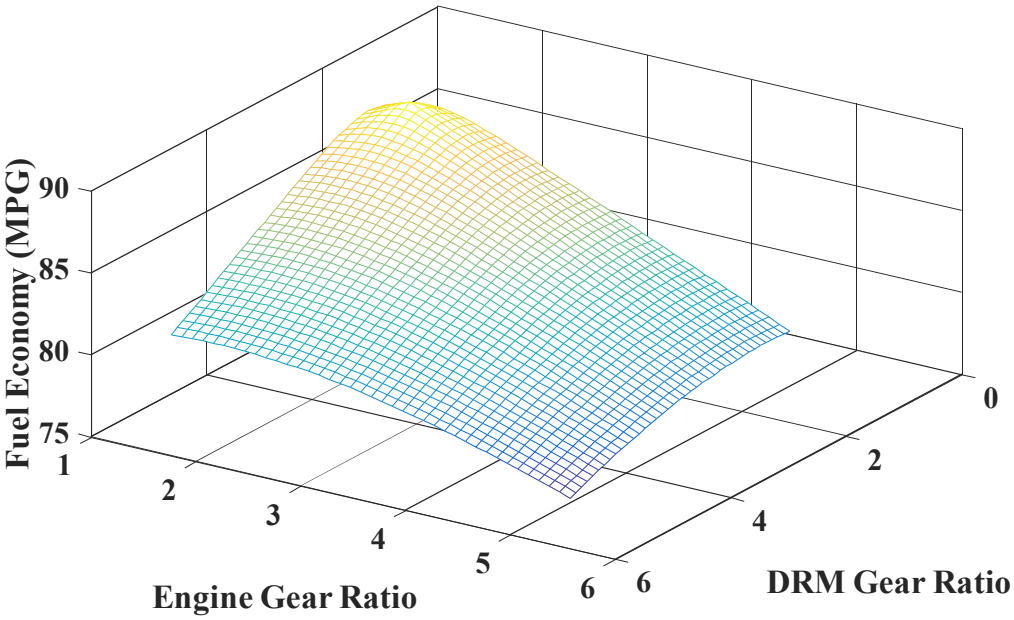

Figure 43 Gear ratio sensitivity for UDDS drive cycle.

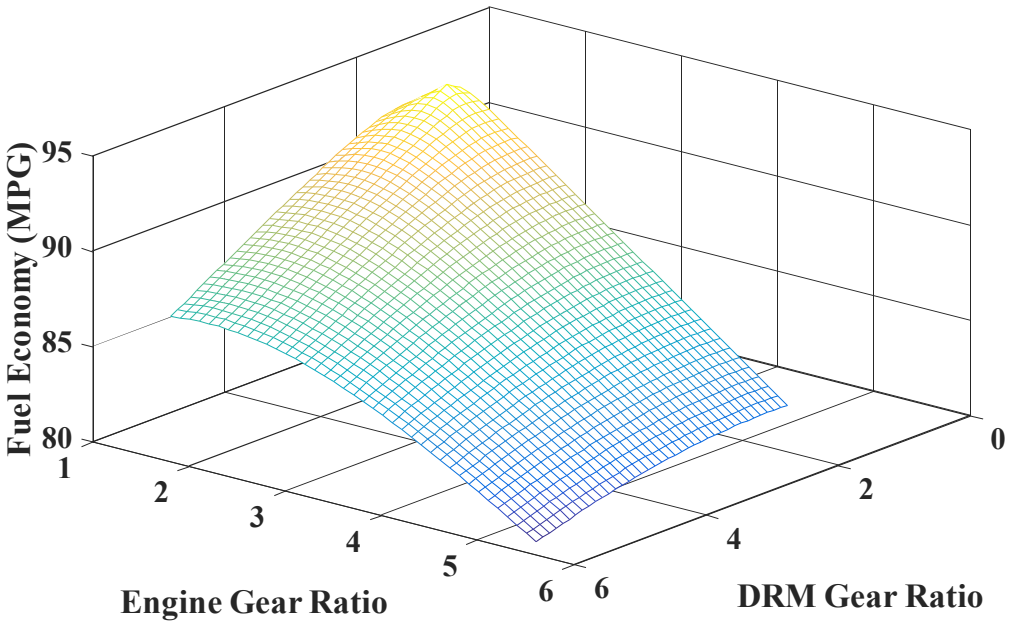

Figure 44 Gear ratio sensitivity for HWFET drive cycle.

The simulation results indicate the optimal design point is the engine gear ratio R_{eng} and DRM gear ratio R_{DRM} are 2.05 and 2.52, respectively.

In this study, there are another two drive cycles, which are the IM_240 and SC03, using this gear ratio sensitivity simulation in order to investigate the best gear ratio for fuel economy potential, Table 10 shows the simulation results for fuel economy comparison.

Table 10 Fuel economy comparison

	HWFET	UDDS	IM240	SC03
StarRotor SP-HEV	94.47 MPG	88.62 MPG	85.71 MPG	91.48 MPG
R_{eng}	2.05	2.08	2.05	2.05
R_{DRM}	2.52	2.66	2.72	2.56

As seen from the maximum fuel economy profile, the engine gear ratio has higher have a little variation around 2.05, through which the engine maximum operation torque line is mirrored close to the maximum operation efficiency area of DRM. The predetermined engine gear is set up 2.05, and then the DRM gear ratio sensitivity to fuel economy is shown in Figure 45. A good trade-off for DRM gear ratio is selected at 2.60.

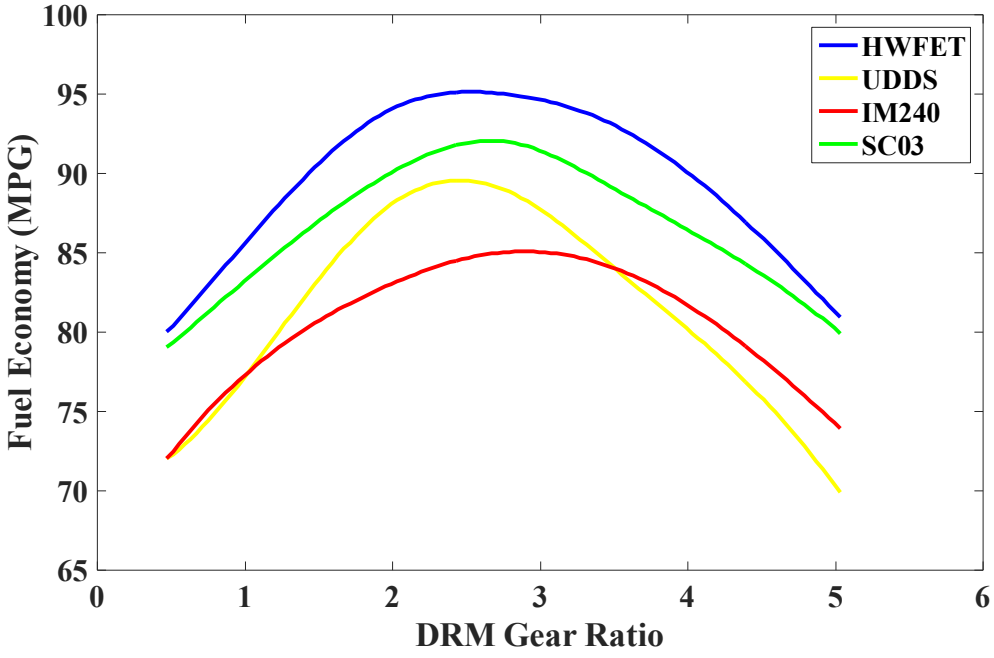

Figure 45 DRM gear ratio sensitivity to fuel economy.

When the DRM gear ratio keeps on increasing from the minimal value, fuel economy is increasing. When the DRM gear ratio value goes to close to the optimal ratio, the fuel economy simulation result starts to bend as the fuel economy is struggling with less improvement. The fuel economy cure shows less upward trend until it reach the maximum value.

Keeping the DRM gear ratio increasing, the fuel economy finally decreases and shows the downward trend. That is because the whole hybrid electric drivetrain is suffering from additional weight and operating mode as parallel hybrid electric drivetrain, but in this type of parallel hybrid electric drivetrain the traction motor more operates as generator unlike in the conventional parallel hybrid electric drivetrain.

The simulation indicates that due to the low torque demand the engine and DRM gear ratios have a significant effect on the fuel economy for the series-parallel EVT drivetrains. This situation could be changed if a high torque demand drive cycle or heavy duty truck is under the study. Therefore for passenger vehicle or low torque demand drive cycle, the fuel economy of the SR–HEV with the series-parallel EVT drivetrain can be further improved by adjusting the DRM gear to 2.6 in order to make StarRotor Engine torque output close to the driven wheels demand of drive cycles.

7.4 Summary

In this chapter, the sensitivity of vehicle performance to engine and DRM gear ratios for a SR–HEV with series-parallel EVT has been analyzed by using dynamic programming. The results generated in this chapter provide helpful guidance for HEV design.

CHAPTER VIII

CONCLUSIONS

In this dissertation, the StarRotor Engine is introduced. Based on StarRotor Engine's unique characteristics, the SR–HEV is proposed. The series, parallel and series-parallel, three different hybrid electric drivetrains, are reviewed and compared. A design philosophy for these three different hybrid electric drivetrains SR–HEV with a minimal size battery pack is proposed.

the dynamic programming is applied to these three different SR–HEVs, the simulation results indicate that the each of SR–HEVs has a great fuel economy potential compared with the conventional ICE based the HEVs, especially for the SR–HEV with series-parallel EVT drivetrain which can achieve EV fuel economy level and the appropriate gear ratios could further improve the fuel economy for this kind drivetrain.

This research also indicates that the series SR–HEV suffers from the additional weight and energy form conversion. The parallel SR–HEV can achieve the high fuel economy which is very close to the series with relatively small add-on. The parallel SR–HEV also shows a promising future.

REFERENCES

1. M. Ehsani, Y. Gao and A. Emadi, *Modern Electric, Hybrid Electric and Fuel Cell Vehicle—Fundamentals, Theory and Design*, Boca Raton, FL: CRC press, 2010.
2. The U.S. Department of Energy, Fuel Economy Guide 2015 [Online] Available: http://www.fueleconomy.gov/feg/pdfs/guides/FEG2015.pdf
3. Teslamotor, Tesla model S, Charging, Adapter Guide [Online] Available: http://www.teslamotors.com/models-charging#/outlet
4. Y. Gao, M. Ehsani, "Design and control methodology of plug-in hybrid electric vehicles," *IEEE Trans. Ind. Electro*, vol. 57, no. 2, pp. 633-640, Jan. 2010.
5. S. G. Wirasingha, N. Schofield and A. Emadi, "Plug-in hybrid electric vehicle developments in the US: trends, barriers, and economic feasibility," *in Proc. IEEE Vehicle Power and Propulsion Conf.*, September, 2008, pp. 1-8.
6. S. S. Williamson, "Electric drive train efficiency analysis based on varied energy system usage for plug-in hybrid electric vehicle application," *in Proc. IEEE Power Electron. Spec. Conf.*, Jun. 2007, pp. 1515-1520.
7. StarRotor Corporation, Compressors, fifth-generation compressor, 2015[Online] Available: http://www.starrotor.com/Compressors/FifthGenerationCompressor
8. M. Holtzapple and A. Rabroker, White paper: StarRotor Engine: A novel power source for the military, StarRotor Corporation, March 2004.
9. A. Rabroker, K. Ross and M. Holtzapple, Proposal: Prototype StarRotor Engine, StarRotor Corporation, Augest 2006.

10. M. Holtzapple, White paper: Electricity production by 1.2-kW StarRotor Engine, StarRotor Corporation, November 2014.
11. R. B. GmbH, *Automotive Handbook*, London: Professional Engineering Pub., 2004.
12. A. Emadi, K. Rajashekara, S. S. Williamson, and S. M. Lukic, "Topological overview of hybrid electric and fuel cell vehicular power system architectures and configurations", *IEEE Trans. Veh. Technol.,* vol. 54, no. 3, pp. 763-770, May 2005.
13. M. Ehsani, Y. Gao and J. M. Miller, "Hybrid electric vehicles: architecture and motor drives," *Proc. IEEE*, vol. 95 no. 4, pp. 719-728, April 2007.
14. C. Lin, H. Peng, J. W. Grizzle, and J. Kang, "Power management strategy for a parallel hybrid electric truck", *IEEE Trans. Cont. syst. Technol.*, vol. 11, no. 6, pp. 839-849, November 2003.
15. S. M. Lukic and A. Emadi, "Effects of drivetrain hybridization on fuel economy and dynamic performance of parallel hybrid electric vehicles," *IEEE Trans. Veh. Technol.*, vol. 53, no. 2, pp. 385-389, March, 2004.
16. A. Sciarretta, M. Back and L. Guzzella, "Optimal control of parallel hybrid electric vehicle," *IEEE Trans. Control Syst. Technol.*, vol.12, no. 3, pp. 352-363, May 2004.
17. L. Chen, F. Zhu, M. Zhang, Y. Huo, C. Yin, and H. Peng, "Design and analysis of an electrical variable transmission for a series-parallel hybrid electric vehicle," *IEEE Trans. Veh. Technol.*, vol. 60, no. 5, pp. 2354–2363, Jun. 2011.
18. L. Chen, X. Gang, and J. Sun, "Torque coordination control during mode transition for a series-parallel hybrid electric vehicle," *IEEE Trans. Veh. Technol.*, vol. 61, no. 7, pp. 2936–2949, Sep. 2012.

19. R. Wohl, T. Long, Jr., V. Mucino, and J. E. Smith, "A model for a planetary-CVT mechanism: analysis and synthesis," in *Proc. SAE Congress Expo.*, Mar. 1993, pp. 1–11.

20. J. Liu, H. Peng, and Z. Filipi, "Modeling and analysis of the Toyota hybrid system," in *Proc. IEEE/ASME Int. Conf. Adv.*, Jul. 2005, pp. 134–139.

21. J. Liu and H. Peng "Model and control of a Power–Split Hybrid Vehicle," *IEEE Trans. Control Syst. Technol*., vol. 16, no. 6, pp. 1242–1251, November 2008

22. K. Muta, M. Yamazaki, and J. Tokieda, "Development of new-generation hybrid system THS II—Drastic improvement of power performance and fuel economy," in *SAE*, Warrendale, PA, Tech. Rep. 2004-01-0064, 2004.

23. M. Duoba, H. Ng, and R. Larsen, "In-situ mapping and analysis of the toyota prius HEV engine," in *SAE*, Warrendale, PA, Tech. Rep. 2000-01-3096, 2000.

24. B. Mashadi and S. A. M. Emadi, "Dual–Mode Power–Split transmission for hybrid electric vehicle," *IEEE Trans. Veh. Technol.*, vol.59, no. 7, pp.3223-3232, Sep. 2010.

25. D. Rizoulis, J. Burl, and J. Beard, "Control strategies for a series-parallel hybrid electric vehicle," in *SAE*, Warrendale, PA, Tech. Rep. 2001-01-1354, 2001.

26. Y. B. Wang, M. Cheng, Y. Fan, and K.T. Chau, "A double-stator permanent magnet brushless machine syste for electric vehicle transmission in hybrid electric vehicles," in *Proc. IEEE VPPC*, 2010, pp. 1-5.

27. L. Xu, "A new breed of electric machines—Basic analysis and applications of dual mechanical port electric machines," in *Proc. 8th Int. Conf. Elect. Mach. Syst.*, 2005, pp. 24–29.

28. Y. Cheng, R. Trigui, C. Espanet, R. Trigui, A. Bouscayrol, and S. Cui, "Specifications and design of a PM electric variable transmission for Toyota Prius II," *IEEE Trans. Veh. Technol.,* vol. 60, no. 9, pp. 4106–4114, Nov, 2011.

29. M. J. Hoeijmakers and M. Rondel, "The electrical variable transmission in a city bus," in *Proc. 35th IEEE PESC*, 2004, pp. 2773–2778.

30. M. J. Hoeijmakers and J. A. Ferreira, "The electric variable transmission," *IEEE Trans. Ind. Appl.*, vol. 42, no. 4, pp. 1092–1093, Jul./Aug. 2006.

31. R. Ghorbani, E. Bibeau, P. Zanetel, and A. Karlis, "Modeling and simulation of a series parallel hybrid electric vehicle using REVS," in *Proc. Rec. Amer.Control Conf.*, 2007, pp. 4413–4418.

32. E. Nordlund and S. Eriksson, "Test and verification of a four-quadranttransducer for HEV applications," in *Proc. IEEE. Veh. Power Propuls. Conf.*, pp. 37–41, 2005.

33. X. Zhu and M. Cheng, "Design, analysis and control of hybrid excited doubly salient stator-permanent-magnet motor," in *SCIENCE CHINA Technological Sciences*, vol. 53, no. 1, pp. 188-199, 2010

34. R. E. Bellman, *Dynamic Programming*. Princeton, NJ: Princeton Univ. Press, 1957.

35. D.P. Bertsekas. *Dynamic Programming and Optimal Control*. Belmont, Mass.: Athena Scientific, 2007.

36. O. Sundström and L. Guzzella, "A generic dynamic programming Matlab function," in *Proc. IEEE Int. Conf. Control Appl*., Jul. 2009, pp. 1625–1630.

37. S. Delprat and T. M. Guerra, "Control strategies for hybrid vehicles: Optimal control," in *Proc. IEEE VTC*, 2002, pp. 1681–1685.

38. Z. Han, Z. Yuan, T. Guangyu, C. Quanshi, and C. Yaobin, “Optimal energy management strategy for hybrid electric vehicles,” in *SAE*, Warrendale, PA, 2004-01-0576, 2004.

39. S. R. Cikanek, K. E. Bailey, and B. K. Powell, “Parallel hybrid electric vehicle dynamic model and powertrain control,” in *Proc. Amer. Control Conf*., Jun. 4-6, 1997, vol. 1, pp. 684–688.

40. S. Delprat, J. Lauber, T. Marie, and J. Rimaux, “Control of a parallel hybrid powertrain: Optimal control,” *IEEE Trans. Veh. Technol.*, vol. 53, no. 5, pp. 872–881, May 2004.

41. A. Brahma, Y. Guezennec, and G. Rizzoni, “Optimal energy management in series hybrid electric vehicles,” in *Proc. Amer. Contr. Conf.*, June 2000.

42. S. Barsali, C. Miulli, and A. Possenti, “A control strategy to minimize fuel consumption of series hybrid electric vehicles,” *IEEE Trans. Energy Convers.*, vol. 19, no. 1, pp. 187–195, Mar. 2004.

43. J. Liu and H. Peng, “Control optimization for a power-split hybrid vehicle,” in *Proc. Amer. Control Conf.*, 2006, pp. 466–471.

44. Y. Cheng, K. Chen, C. C. Chan, A. Bouscayrol, and S. Cui, “Global modelling and control strategy simulation for a hybrid electric vehicle using electrical variable transmission,” *IEEE Veh. Technol. Mag*., vol. 4, no. 2, pp. 73–79, Jun. 2009.

45. Y. Cheng, C. Espanet, R. Trigui, A. Bouscayrol, and S. Cui, “Design of a permanent magnet electric variable transmission for HEV application,” in *Proc. IEEE VPPC*, Sep. 1–3, 2010, pp. 1–5.

46. B. Conlon, “Comparative analysis of single and combined hybrid electrically variable transmission operating modes,” in *SAE*, Warrendale, PA, Tech. Rep. 2005-01-1162, 2005

47. E. Vinot, R. Trigui, Y. Cheng, A. Bouscayrol, and C. Espanet, “Optimal management and comparison of SP-HEV vehicles using the dynamic programming method,” in *Proc. IEEE VPPC*, Oct. 10–12, 2012, pp. 944–949.

48. United States Environmental Protection Agency, Transportation and air quality, Modeling, Testing &Research, Testing & Measuring Emissions, Dynamometer Drive Aid, October 2015 [Online]
Available: http://www3.epa.gov/nvfel/testing/dynamometer.htm,

49. K. E. Bailey and B. K. Powell, “A hybrid electric vehicle powertrain dynamic model,” in *Proc. Amer. Control Conf.*, Jun. 1995, pp. 1677–1682.

50. K. L. Butler, M. Ehsani, and P. Kamath, “A matlab-based modeling and simulation package for electric and hybrid electric vehicle design,” *IEEE Trans. Veh. Technol.*, vol. 48, no. 6, pp. 1770–1778, Nov. 1999.

51. B. K. Powell, K. E. Bailey, and S. R. Cikanek, “Dynamic modeling and control of hybrid electric vehicle powertrain systems,” *IEEE Control Syst. Mag.*, vol. 18, no. 5, pp. 17–33, Oct. 1998.